NOLTR 69-151

MEASUREMENTS OF BLAST-INDUCED TRANSIENT PRESSURES AT THE BASE OF A CONE IN SUPERSONIC FLOW

By
Frank P. Baltakis
Gary D. Senechal

5 NOVEMBER 1969

NOL

UNITED STATES NAVAL ORDNANCE LABORATORY, WHITE OAK, MARYLAND

NOLTR 69-151

MEASUREMENTS OF BLAST-INDUCED TRANSIENT PRESSURES AT THE BASE OF A CONE IN SUPERSONIC FLOW

Prepared by:
Frank P. Baltakis
Gary D. Senechal

ABSTRACT: Transient pressures, induced by a head-on blast wave, have been measured at the base of a nine-degree half-angle cone in a supersonic stream using a wind-tunnel shocktube technique. Tests were conducted at free-stream Mach numbers of 3, 5 and 6.5 and at blast wave Mach numbers of 1.5 to 3, 2 to 5 and 4 to 8 at free-stream Mach numbers of 3, 5 and 6.5, respectively. Within the range of this experiment, the shock-induced base pressure was found to increase approximately in proportion to the blast wave Mach number squared. When expressed in ratio to the free-stream static pressure, the induced base pressure was found to decrease, approximately, linearly with increasing free-stream Mach number. At the free-stream/blast wave Mach number conditions of 3/3, 5/5 and 6.5/8 the respective induced base pressure to initial free-stream static pressure ratios were 5, 8 and 18.

NOLTR 69-151 5 November 1969

MEASUREMENTS OF BLAST-INDUCED TRANSIENT PRESSURES AT THE BASE OF A CONE IN SUPERSONIC FLOW

This study was conducted to obtain design information related to shock-induced transient pressures at the base of a re-entry vehicle body type. The results of this study are the first of its kind; therefore, no comparisons are possible with other analytical or experimental studies. The relations indicated here are approximate and should not be used indiscriminately outside of the range of flow conditions for this experiment. Funding for this study was provided by the Defense Atomic Support Agency under Task NOL 161-DASA.

Contributions of Mr. Benjamin J. Crapo, who assisted in the development of electronic instrumentation components, and those of Mr. Bernard S. Hull, who provided shocktube diaphragms, are gratefully acknowledged.

GEORGE G. BALL
Captain, USN
Commander

L. H. SCHINDEL
By direction

CONTENTS

ILLUSTRATIONS

ILLUSTRATIONS (Cont.)

ILLUSTRATIONS (Cont.)

TABLES

BLANK PAGE

INTRODUCTION

A re-entry vehicle, passing through a blast wave, may experience severe transient pressures. On windward surfaces such pressures may be caused by blast wave vehicle-shock interactions. At the base, on the other hand, severe transient pressures may result from an implosion of the blast wave.

Shock interaction effects on windward facing surfaces have been investigated analytically, numerically and experimentally. A recent review of such results may be found in Reference (1). The base region, to date, has received very little attention because the pressures acting on the base are normally very low initially and the induced transient pressures are not expected to be excessively large, in general. Also, this region of the body is an indication of one of the more difficult problem studies. In this regard, analytical or numerical analyses are complicated by nonuniformities of the near wake flow, and by the complex structure of the blast wave after it passes through the vehicle's shock layer. Prior to this study method, there has not been any analytical or experimental information which would predict blast wave induced transient pressures experienced at the base of a body in such an environment.

This paper describes an experimental study of the transient pressures measured at the base of a nine-degree semi-angle cone body. The study has been concerned with the head-on shock case only (i.e., the model at zero angle of attack) since at this condition the implosion of the blast wave is expected to be most intense. The wind-tunnel shocktube technique, which had been developed at the Naval Ordnance Laboratory (NOL) for an earlier shock-interaction program, was used for this investigation.

SYMBOLS

c	chord length of the side strut measured parallel to the free-stream flow
C_{P_b}	base-pressure coefficient, $\frac{P_b - P_\infty}{q}$
ΔC_{P_b}	change in base-pressure coefficient (see Fig. 8)

D	gage diameter
M	Mach number
M_1	free-stream Mach number prior to interaction
M_s	shock Mach number relative to the flow
M_{sg}	shock Mach number at the periphery of the gage (see Fig. 11)
n	number of side struts
P	shock-induced peak pressure
P_a	ambient pressure
$P_{D=0.1}$	pressure indicated by a gage of diameter D=0.1 in.
P_∞	free-stream static pressure, prior to interaction
ΔP	shock-induced overpressure
t	side strut maximum thickness

TEST FACILITY

WIND-TUNNEL SHOCKTUBE APPARATUS

Tests were performed in the NOL Supersonic Tunnel No. 1 which is an open-jet, blowdown wind-tunnel facility. The tunnel operates on air drawn in at atmospheric pressure and temperature; this is discharged into a 52-foot-diameter vacuum sphere.

For this particular experiment, the tunnel was modified whereby it was fitted with three conical nozzles, a matched diffuser and a shocktube.

The shocktube (a 1.5-inch I.D. by 12-foot-long steel tube) was installed in the tunnel reservoir aligned coaxially with the nozzles. The discharge end of this tube was positioned about four

inches upstream of the main nozzle throat. The driven section of the tube was left open so that it contained air at tunnel supply conditions. The driver section itself was pressurized with air or helium. Aluminum bursting diaphragms, ranging from 0.02 to 0.07 inch in thickness were used in the shocktube. To facilitate reloading of the diaphragms, a 70-degree bend over a 34-inch radius was made into the driver section which, as may be seen in Figure 1, permitted the location of the partition section outside of the main tunnel. Nozzle geometry information will be found in Table 1.

FLOW CONDITIONS

Free-stream flow conditions, to which the model was exposed prior to blast wave impingement, are listed in Table 1. Since the nozzles were conical in shape, Table 1 lists Mach number values for the nozzle exit and the axially measured gradients in the test section. These measurements were obtained by Pitot pressure surveys. The air supply pressure and temperature for all three nozzles were 14.6 psia and 70°F (±5°F), respectively; however, the air dew temperature ranged from -25°F to -50°F.

Shock intensity ranges at different free-stream conditions are also listed in Table 1. The intensities are expressed in terms of shock Mach number relative to the free-stream flow.

A parameter of considerable interest was the quality of the flow behind the blast wave. This was investigated in an earlier experiment and is reported in Reference (2). The study found that the flow behind the blast wave is more uniform in the conical nozzles (provided the divergence angle was small) than it was in contoured nozzles. The study also showed that the flow was quite uniform at low blast wave intensities; but that the duration and quality of the flow deteriorated rapidly as the blast wave Mach number exceeded the value for the nozzle flow.

MODEL CONFIGURATIONS

The model chosen for this study was a nine-degree semi-angle cone having a three-inch base diameter. During tests it was supported in the tunnel on a thin, streamlined strut, as illustrated on Figures 2 and 3.

Two additional model support configurations were also used for the purpose of assessing the effects of model supports. One configuration consisted of multiple side struts attached to the model as shown on Figures 2 and 4. The other configuration was a

three-prong type of axial support attached to the base of the model as shown on Figure 5. The individual rods used in this configuration were 3/8 inch in diameter and were fitted around the model base on a one-inch radius circle.

INSTRUMENTATION

OPTICAL SETUP

Optical measurements made in this investigation served two purposes: (1) to indicate the condition of the blast wave; and (2) to provide data for blast wave intensity determination. Blast wave intensity was determined by means of time and distance measurements. For this experiment a two-spark shadowgraph system was used to record the wave patterns at two positions in the test section. The time interval measured here was obtained by means of a phototube and a time interval meter (Berkeley counter with a 1/10-microsecond count). This particular optical setup is illustrated on Figure 6.

Sparks for photographs were generated by two pairs of electrodes which were located along a common optical axis. The light from the sparks was reflected from a parabolic mirror through the test section onto a large (11 x 14 in.) photographic plate where the wave patterns were recorded.

PRESSURE TRANSDUCERS

The transducers used to measure the transient pressures were produced within the Laboratory. The design concept for these transducers was developed at the Laboratory in conjunction with an earlier shock-interaction study program. Reference (3) describes the design and performance characteristics of these in some detail. In brief, the transducer utilizes a piezoelectric crystal supported on an acoustically matched slender rod. These transducers have a response time which is less than one microsecond; also, the pressure sensing element is only 0.093 inch in diameter.

Figures 2 and 4 show transducer locations on the model. These elements were soft mounted in a removable base plate, and a smooth transition was ensured at the surface junction.

Transducer outputs were amplified, displayed on Tektronix 535 oscilloscopes, and recorded using Polaroid cameras. The outputs were amplified by means of miniature amplifiers (Model 401A, made by pcb Piezotronics, Inc.) which were located within the model itself.

Transducer calibrations were performed using a special shocktube having a rectangular cross section. The shocktube and the calibration method are described in Reference (3).

RESULTS AND DISCUSSION

PRELIMINARY MEASUREMENTS

Static Base-Pressure Measurements. Static base-pressure measurements were made to ensure that the model support and flow divergence (since the nozzles were conical) did not significantly affect the initial base pressures. The results from these measurements are found on Figures 7 and 8.

Figure 7 shows the measured values for all three nozzles and compares these with data from References (4) and (5). It is seen that at a free-stream Mach number of 3, the measurements are approximately in agreement with the values predicted for a cone having a turbulent boundary layer. However, at Mach numbers of 5 and 6.5, the measurements are in agreement with the values predicted for a cone with a laminar boundary layer.

Base-pressure coefficients for all three cases are slightly higher than those predicted in References (4) and (5). These differences are presumed to be caused by the model supports. To assess the magnitude of this latter effect, additional measurements were made using model support configurations B and C (see Fig. 2). The results from these measurements, which are shown in Figure 8, indicate that the base-pressure coefficient increases (the base-pressure decreases) as the number of supports is increased. Extrapolation to a zero number of supports would indicate that the basic, single strut support (configuration A) causes an increase in the model base pressure of about eight percent. An equation, derived for a cone with multiple fins (Ref. (4)), was used as a guide for the extrapolation.

Shock-Induced Pressures Under Wind-Off Conditions. A few preliminary shocktube test shots were made with the model located in the tunnel, but in a wind-off atmospheric pressure condition. For these preliminary tests the air density in the model base region was high and the character of the blast wave, as it imploded over the base region, could be readily observed (optically). Also, the shock-induced pressures, for this case, were high and could be measured quite accurately at any point on the model's base.

One two-spark shadowgraph and a set of pressure-time traces for a typical wind-off case are shown on Figure 9. It can be seen there that the portion of the blast wave which is adjacent to the base is essentially cylindrical in shape. For such a cylindrical implosion, Chisnell (Ref. (6)) has developed a method which allows one to predict shock characteristics analytically. This theory was used herein to calculate the peak pressure variation along the radius of the model base for comparing with the experimental measurements. It may be seen, from Figure 10, that the measured and computed variations between stations 2 and 3 are in very good agreement.

At the center of the base, theoretically, the peak pressure should approach infinity. The measured value, because of the finite size of the pressure transducer, necessarily represents a certain average pressure. The degree to which the size of the transducer influences the measurement at the center has been checked analytically and is illustrated on Figure 11. It is seen that the measured pressure depends on the intensity of the imploding wave as well as it depends on the diameter of the gage. A reduction, for example, in the diameter of the present gage by a factor of three would increase the measured value by about 35 percent.

Model Support Effects on Base Overpressure. Effects of the model support on shock-induced overpressures were difficult to determine precisely, either analytically or experimentally. The method which was finally adopted here was based on a comparison of measurements taken with different strut configurations. The configurations which were used included the basic single strut alone, and the same basic strut with one and two dummy struts added, as shown on Figure 2.

The comparison noted above was made at a free-stream Mach number of 5, and at blast wave Mach numbers ranging from about 2.5 to 4.

The results, which are summarized on Figure 12, show that the peak overpressure (measured at the center of the base) decreases as the number of struts is increased. The curve-fitted values at a blast wave Mach number of 3.5 are shown replotted on Figure 13. An extrapolation of this curve indicates that the overpressures for a model free of side supports would be about 33 percent larger than those for a model supported by the basic single side strut alone.

Another method of model support consisted of three 3/16-inch-diameter rods attached to the model base as shown on Figure 5. This scheme was also tried during the investigation but was abandoned since the measured peak overpressures were considerably larger and resulted in data containing more scatter than those for the simpler side support. Shadowgraphs taken at wind-off conditions showed that strong reflections of the imploding wave were produced by these rods.

SHOCK-INTERACTION PRESSURE DATA

Pressure-Time Traces. Figure 14 is composed of several Polaroid pictures of the pressure-time traces made at different flow conditions. These traces are typical and are included here to illustrate the nature of the raw data acquired during this study.

It may be seen that for a free-stream Mach number of 3 (Fig. 14-A) the signal trace deflections are large and the pressure magnitudes are readable, quantitatively, at all three stations. However, at larger free-stream Mach number, because of the lower initial base pressures, the trace deflections at stations 2 and 3 are quite small. Data at these stations were used for qualitative analysis only.

On Figures 15-A through 15-E, the pressure-time variations are plotted to the same scale for all three model stations. The zero time in these graphs corresponds to the arrival time of the shock at station 3 (see Fig. 2); and the zero pressure corresponds to the measured base pressure prior to the interaction. Figure 15-A, for example, shows that at a free-stream Mach number of 3.1 and a blast wave Mach number of 1.5 the imploding shock at station 3 induces an overpressure of about 0.04 psi.. About 16 microseconds later the shock reaches station 2 where it induces an overpressure of about 0.06 psi. After about 20 additional microseconds, the shock implodes and is reflected at the base center inducing an overpressure of approximately 0.34 psi. The reflected shock subsequently passes stations 2 and 3 at about 12 and 25 microseconds later, respectively.

Figure 15-B shows a pressure-time history at the same free-stream Mach number, but at an increased blast wave Mach number (M_s = 2.36). The pattern here is similar to that noted earlier, but the pressure magnitudes are considerably larger. In a like manner, Figures 15-C, D and E illustrate pressure-time histories made at free-stream Mach numbers of 5 and 6.5. (At a Mach number of 6.5 only station 1 is included since at stations 2 and 3 the pressures were too low for reproduction to any reasonable degree of accuracy.)

Peak Overpressures. The measured peak pressure data are summarized in Table 2. These measured values are listed as overpressures, and are presented in ratio to the preblast free-stream static pressure. For purposes of discussion and illustration, these data are also presented graphically on Figures 16 through 19.

Figure 16 shows the variation in measured overpressures versus blast wave intensity. In addition, the experimental points are shown reproduced on several second-degree polynomial curves. These curves are included primarily to illustrate the data trend. The constants for these polynomials were determined by means of a least squares fit, applied to the experimental data; the overall second-order characteristic was assumed. It can be seen from the Figure that within the range of this experiment the base overpressures increase (approximately) in proportion to the blast wave Mach number squared.

Precise correlation of these data, with empirical relations, was not possible herein because of the considerable scatter for the results. Some of this scatter has resulted from imperfections in shock-intensity measurements. Most of the scatter, however, was estimated to be the consequence of irregularities in the blast wave and the resulting eccentricities of the imploding wave. To substantiate this conjecture, data acquired at a free-stream Mach number of 3 were integrated to obtain momentum values which were induced by the collapsing shock. Figure 17 shows such data for transducer stations 1 and 2 (at the base center and at 1/4-inch away from the center, respectively). It can be seen that the scatter here is rather small. This is particularly true when one notes that Figure 17 includes a number of runs which, because of the large eccentricities which are apparent from the pressure traces, were not included in Figure 16. The fact that eccentricities do not significantly affect the induced momentum values can be demonstrated from Figure 17 by noting the small difference between the momentum values at stations 1 and 2.

Figure 18 shows the shock-induced base pressures as multiples of the preblast free-stream static pressure. Here, again, the overall trends are indicated by the second-degree polynomials obtained in the manner described earlier.

To indicate the influence of free-stream Mach number, data from Figure 18 have been replotted on Figure 19. Here, it is seen that the ratio of induced to free-stream static pressure diminishes with increasing free-stream Mach number. These empirical curves (shown) indicate that the variation is approximately inversely proportional to the free-stream Mach number.

SHADOWGRAPHS

Figure 20 shows a number of typical shadowgraph photographs. The tip of the model is not visible here since it is inside of the conical nozzle. The direction of flow in the tunnel (and of the blast wave) is from right to left on the photograph. The reason that the blast wave appears in two places is that the photograph was made using the two-spark system.

Unfortunately, the density in the cone's base region was very low and the shadowgraphs did not show the interactions in detail. The shadowgraphs, nevertheless, do show the condition of the blast wave; the effects of the interaction with the model bow wave and the boundary layer; and, the conditions for the flow field behind the blast wave. For example, at low blast wave intensities (Figs. 20-A and 20-G) the interactions with the model bow wave, and the boundary layer, is weak; the blast wave in the vicinity of the bow wave and the boundary layer remains essentially undisturbed. At high intensities (Figs. 20-N, 20-O and 20-P) the blast wave near the model's surface becomes bifurcated. As pointed out earlier, an increased scatter in the pressure data can be attributed primarily to the effects of this interaction.

CONCLUSIONS

Transient pressures induced by a head-on blast wave have been measured at the base of a nine-degree semi-angle cone at free-stream Mach numbers of 3, 5 and 6.5. Values of blast wave Mach number ranged from 1.5 to 3, 2 to 5, and 4 to 8 at the free-stream Mach numbers of 3, 5 and 6.5, respectively.

The model was supported in the tunnel test section by means of a thin side strut. Pressure measurements indicated that the side strut had caused an increase in the initial, preblast base pressure by about 10 percent, and had reduced the shock-induced transient pressure by about 30 percent.

Peak pressure data obtained during this investigation actually represent average pressures acting over a 0.093-inch-diameter circle (the transducer face area) on the model base. A theoretical estimate of this variation of pressure with the diameter is included herein.

The transient pressure data contain a considerable degree of scatter. This scatter can be attributed, primarily, to eccentricities of the imploding blast wave.

Within the range of this experiment, the shock-induced pressures were found to increase approximately in proportion to the blast wave Mach number squared. When the pressures are given in ratio to the free-stream static pressure, the induced pressures were found to decrease in an approximate linear fashion with increasing free-stream Mach number.

At the free-stream/blast wave Mach number conditions of 3/3, 5/5 and 6.5/8 the corresponding induced base to initial free-stream pressure ratios were 5, 8 and 18, respectively.

REFERENCES

(1) Merritt, D. L., Williams J. and Dawson, P., "Shock Interaction Handbook," NOL Technical Report to be published
(2) Baltakis, F. P., Merritt, D. L. and Aronson, P. M., "Two Techniques for Simulating the Interaction of a Supersonic Vehicle with a Blast Wave." NOLTR 67-154, Oct 1967
(3) Baltakis, F. P., "Development of a Fast-Response Pressure Transducer," NOLTR 69-158, 1969
(4) Honeywell, E. E., "Compilation of Power-Off Base Drag Data and Empirical Methods for Predicting Power-Off Base Drag," TM 334-337, Convair/Pomona, 1959
(5) Darling, J. A., Private communication
(6) Chisnell, R. F., "The Motion of Shock Wave in a Channel with Applications to Cylindrical and Spherical Shock Waves," Journal of Fluid Mechanics, Vol 2, pp 286-298, 1957

Table 1

NOZZLE GEOMETRY AND FLOW CHARACTERISTICS DATA

Mach No. (At nozzle exit)	Axial Mach No. Gradient (per inch)	Exit Diameter (inches)	Throat Diameter (inches)	Length (inches)	Reynolds Number (10^6 per foot)	Range of Blast Wave Mach No.
3.045	0.0248	9.0	4.12	60	2.20	1.5 to 3
5.03	0.0294	12.5	2.27	60	0.89	1.9 to 5.2
6.40	0.056	12.5	1.44	60	0.53	4.3 to 7.9

Table 2

SHOCK-INDUCED TRANSIENT PRESSURES AT THE CENTER OF A NINE-DEGREE CONE

Run	M_1	M_s	ΔP psi	P_p/P_∞
479	3.1	2.84	1.64	4.90
480		2.96	2.01	5.95
481		2.84	1.73	5.18
483		1.58	0.54	1.76
485		1.63	0.43	1.43
486		1.63	0.47	1.54
543		2.36	1.23	3.87
553		1.49	0.35	1.23
593		2.91	1.45	4.51
594	↓	2.91	1.52	4.73
497	5.07	3.52	.094	4.16
499		4.04	.120	5.16
500		4.04	.115	4.95
554		2.25	.048	2.38
555		2.37	.052	2.55
556		2.37	.053	2.59
557		1.90	.033	1.77
559		4.21	.100	4.41
560		3.25	.074	3.42
561		3.61	.091	4.09
562		3.30	.072	3.33
563		3.52	.090	4.03
564		3.08	.068	3.18
565		3.64	.101	4.47
566		3.62	.087	3.90
568		5.13	.132	5.71
569		5.17	.129	5.57
570		5.03	.137	5.90
571		5.00	.128	5.55
687		3.65	.082	3.70
688		3.65	.090	4.04
689	↓	3.93	.099	4.41

Run	M_1	M_s	ΔP psi	P_p/P_∞
710	5.07	3.80	.135	5.91
711		3.55	.111	4.90
712		4.14	.136	5.94
713		2.04	.040	1.96
714		4.13	.135	5.91
715		3.68	.118	5.18
716		3.85	.131	5.75
717	↓	3.40	.100	4.47
574	6.5	7.87	.106	19.6
576		7.18	.056	10.5
577		7.56	.064	12.1
579		7.20	.052	9.94
580		7.48	.058	10.9
582		6.16	.062	11.6
584		4.44	.044	8.39
585		5.98	.069	12.9
587	↓	4.31	.038	7.42

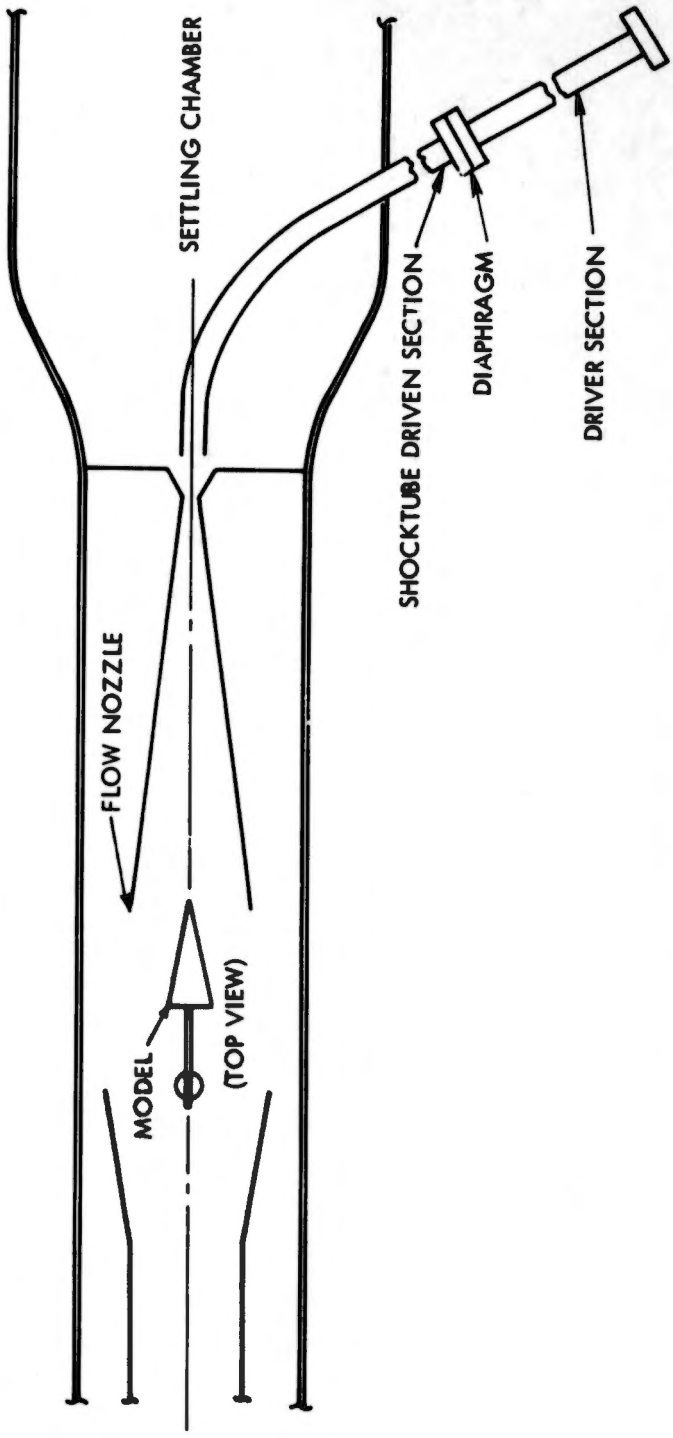

FIG. 1 WIND TUNNEL-SHOCKTUBE TEST SETUP

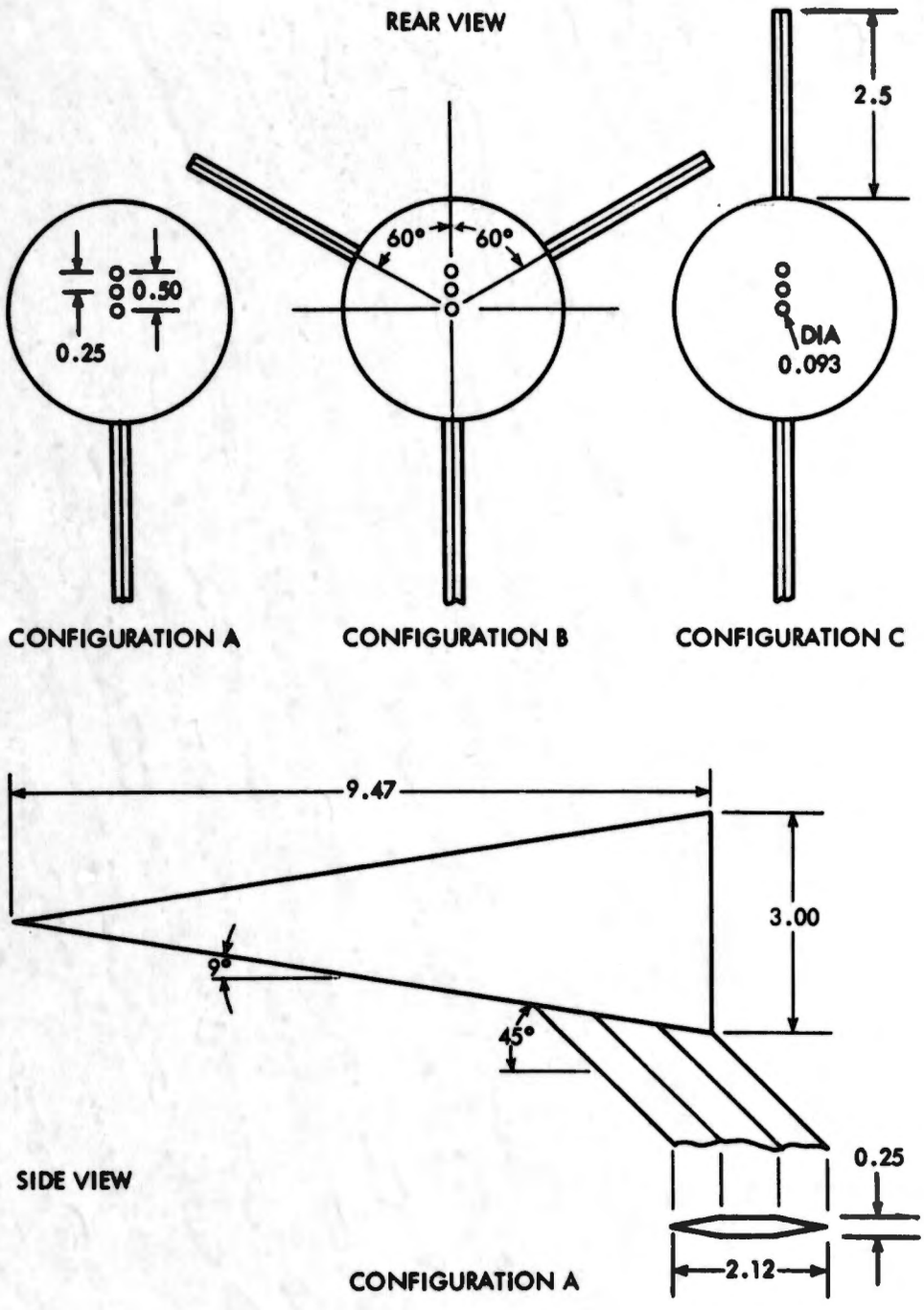

FIG. 2 MODEL AND STRUT GEOMETRY

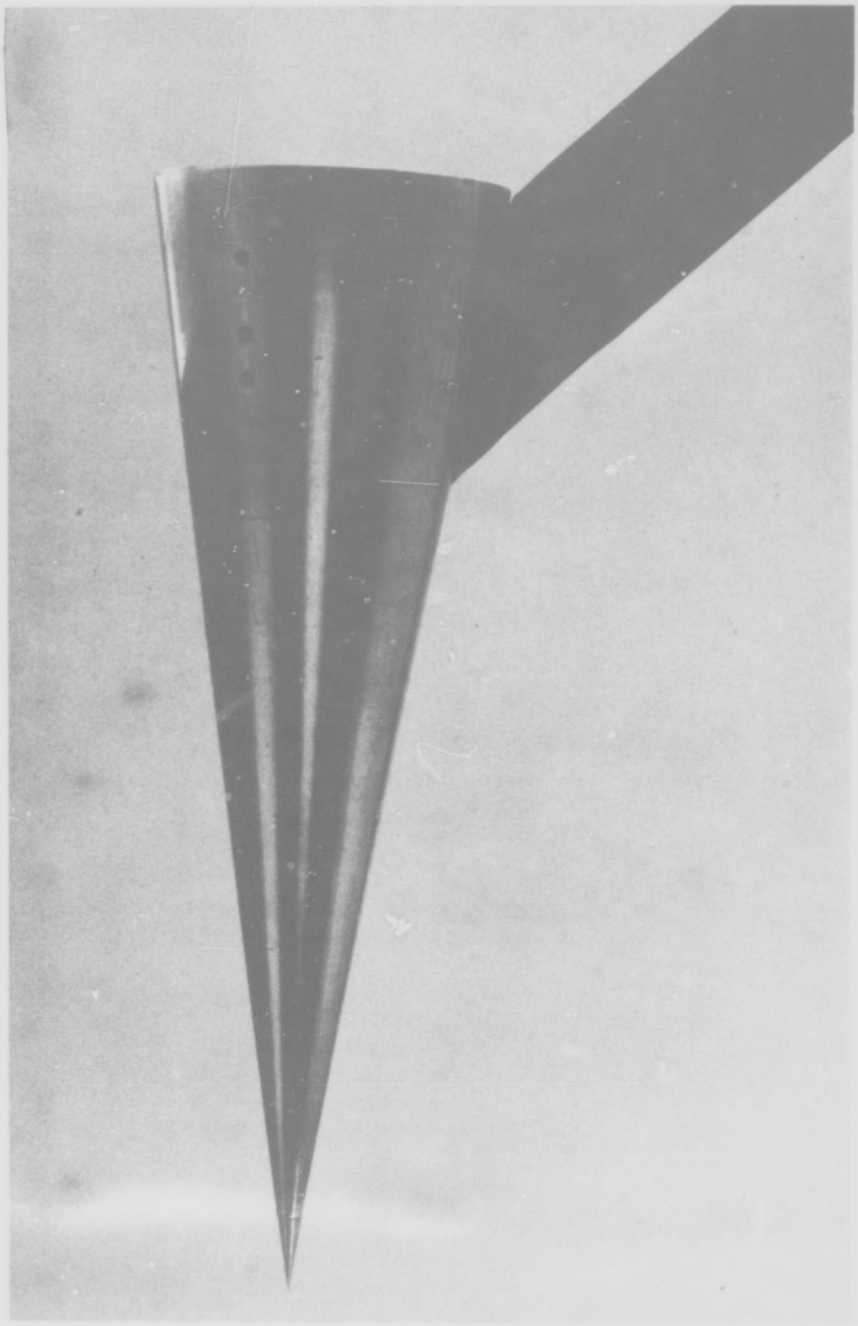

FIG. 3 TEST MODEL PHOTOGRAPH

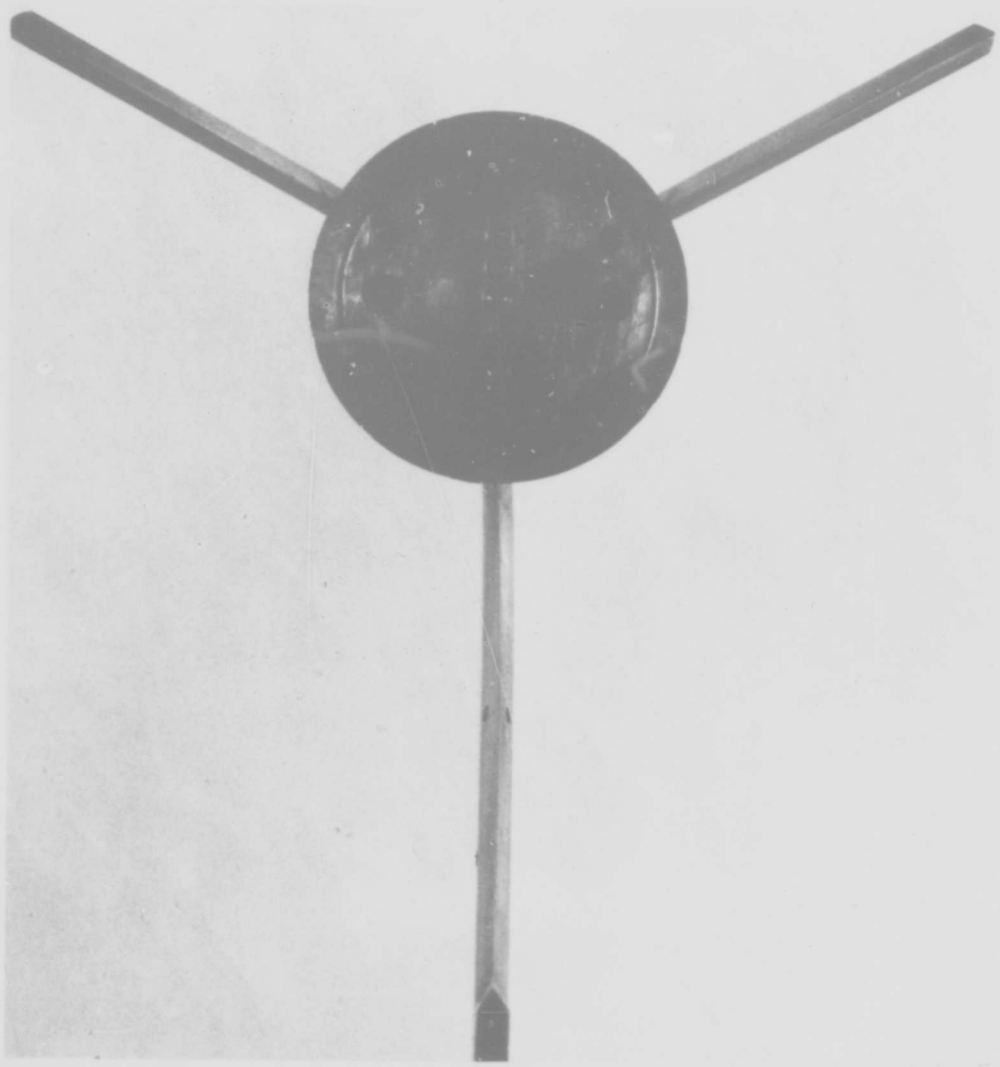

FIG. 4 PHOTOGRAPH OF A MODEL WITH SIMULATED MULTIPLE SIDE STRUTS

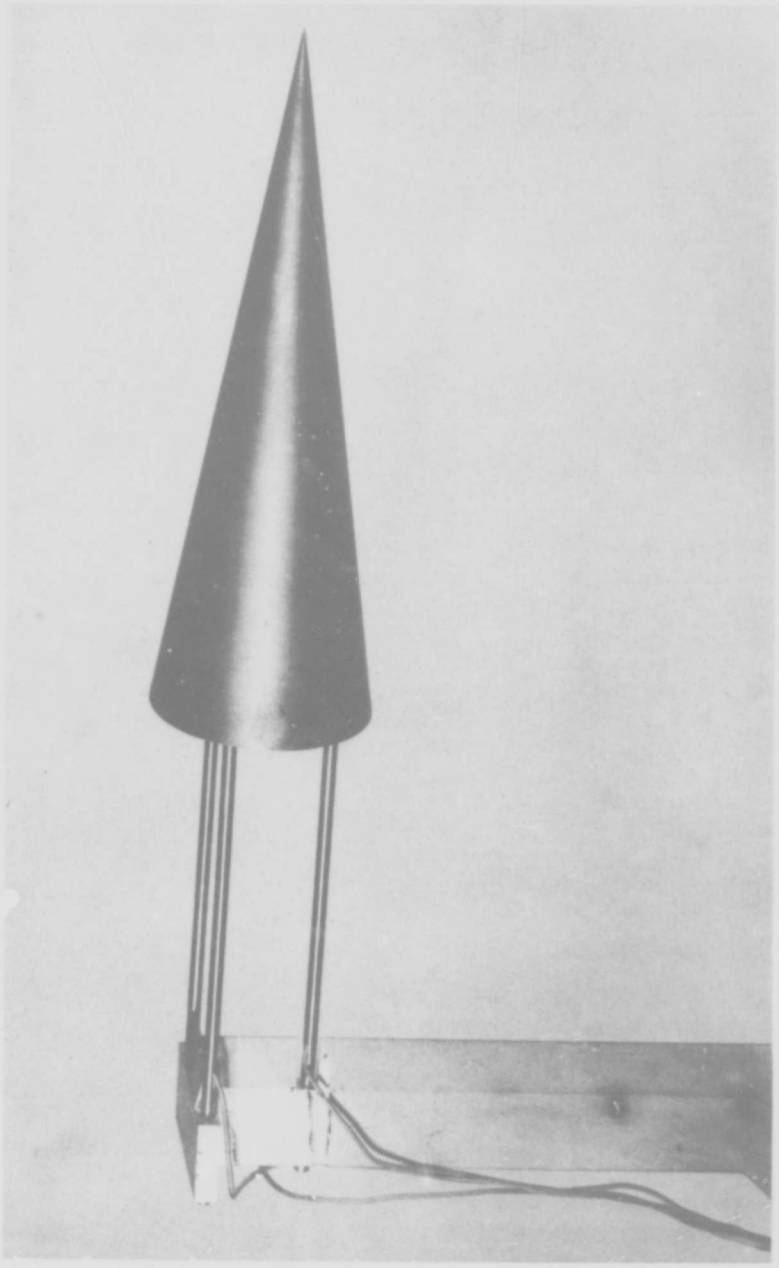

FIG. 5 PHOTOGRAPH OF A MODEL SUPPORTED ON THREE END RODS

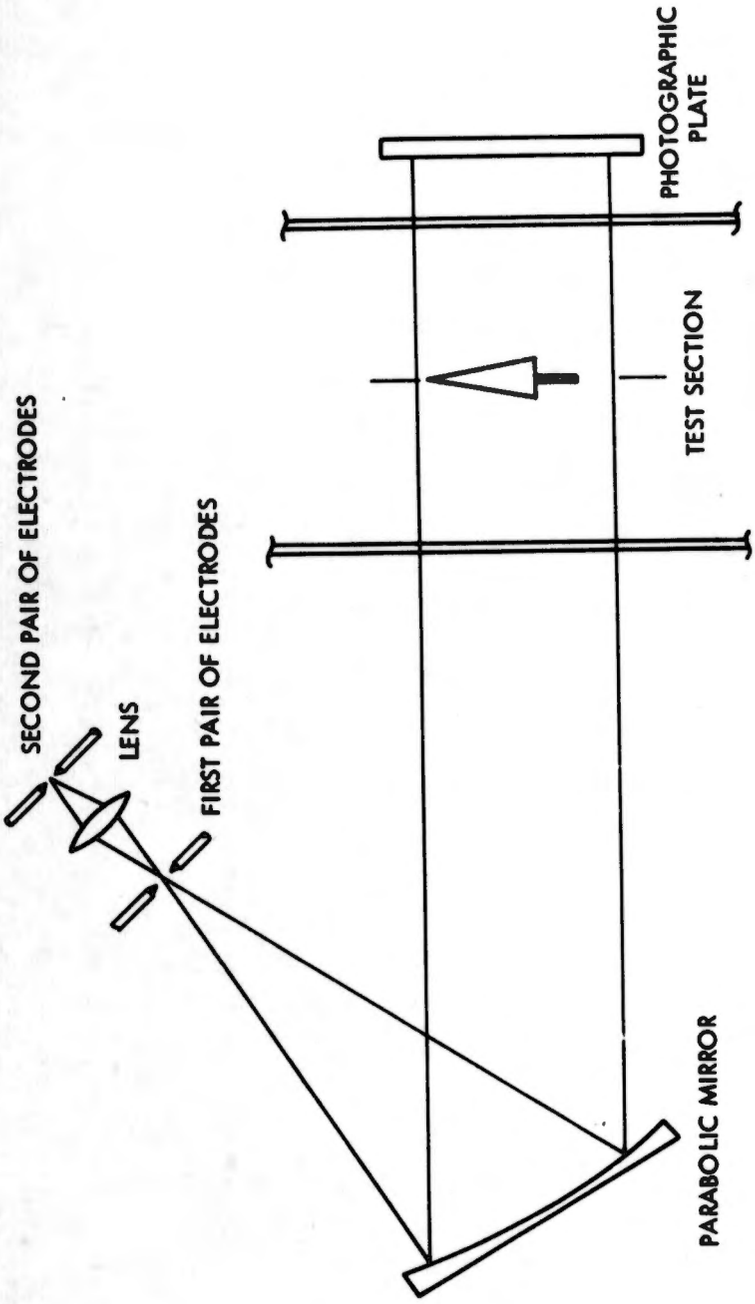

FIG. 6 THE TWO-SPARK SHADOWGRAPH SYSTEM

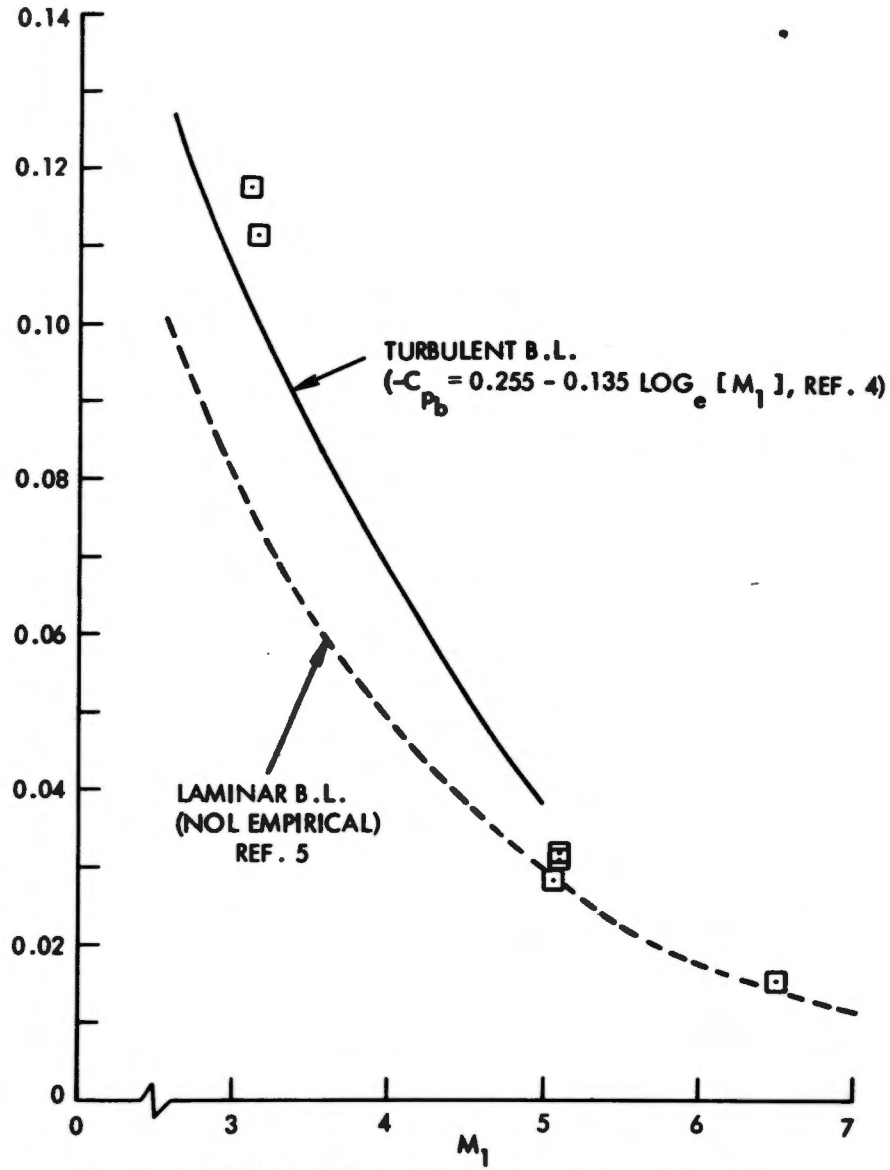

FIG. 7 BASE PRESSURE COEFFICIENT VERSUS FREE-STREAM MACH NUMBER FOR A 9° SEMI-ANGLE CONE

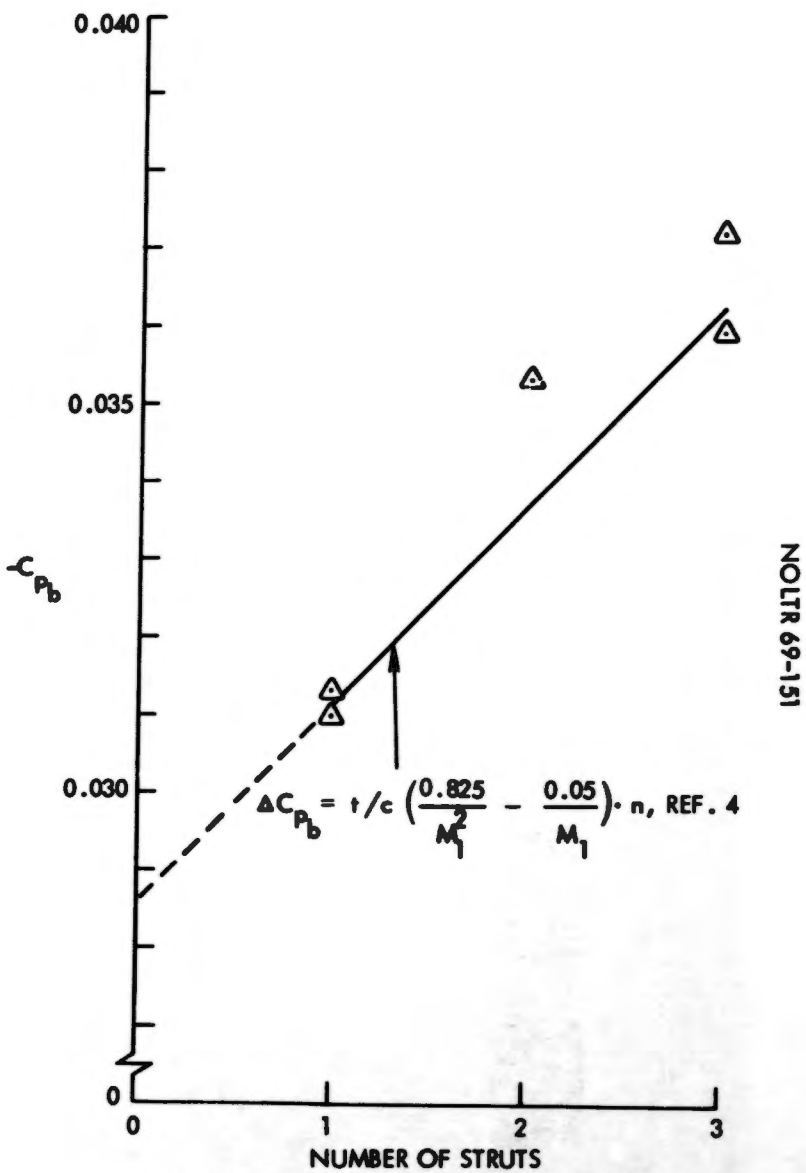

FIG. 8 BASE PRESSURE COEFFICIENT VERSUS NUMBER OF SIDE STRUTS FOR A 9° SEMI-ANGLE CONE AT MACH 5.1

NOLTR 69-151

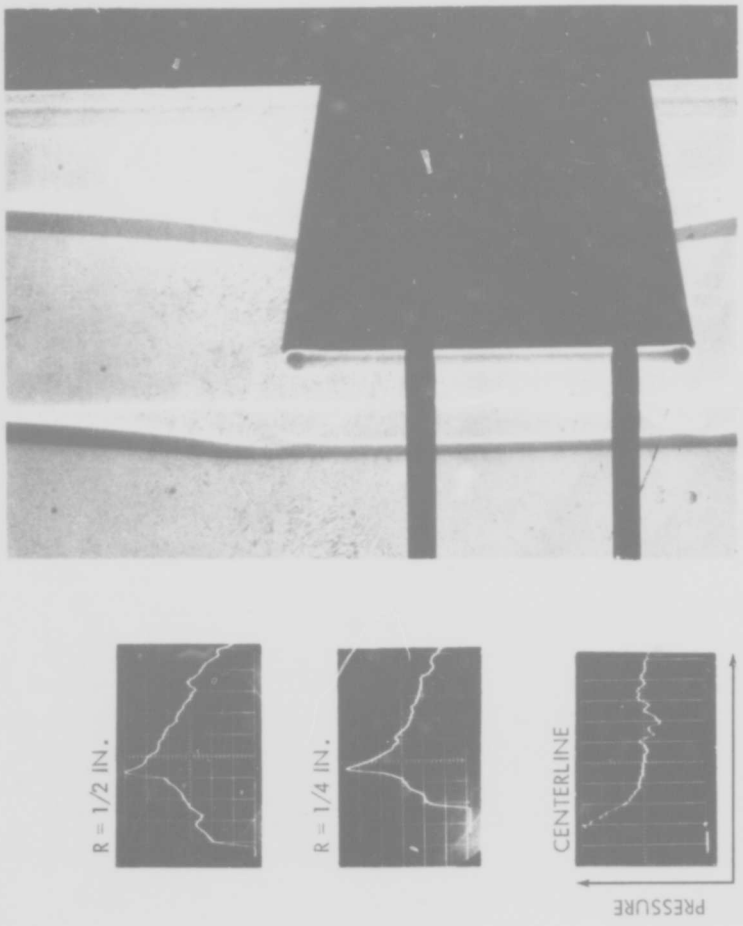

FIG. 9 SHOCK IMPLOSION AT THE BASE OF A 9° CONE IN A QUIESCENT AIR

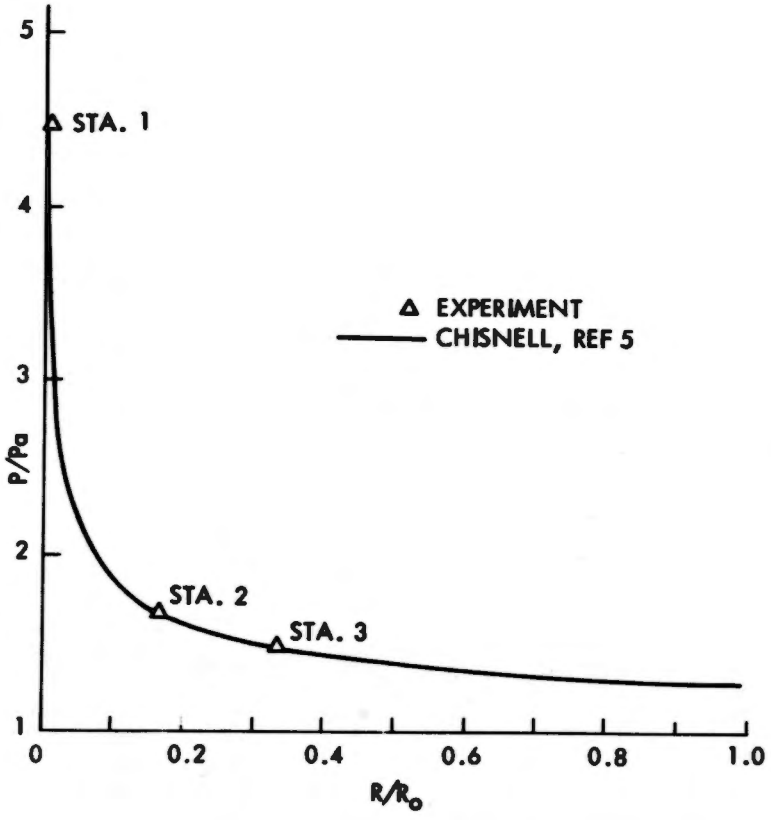

FIG. 10 SHOCK INDUCED PRESSURE VARIATION OVER THE CONE BASE AT WIND-OFF CONDITIONS. $M_s = 1.59$; INITIAL PRESSURE, Pa = 14.38 PSIA; BASE RADIUS, $R_o = 1.5$ IN.

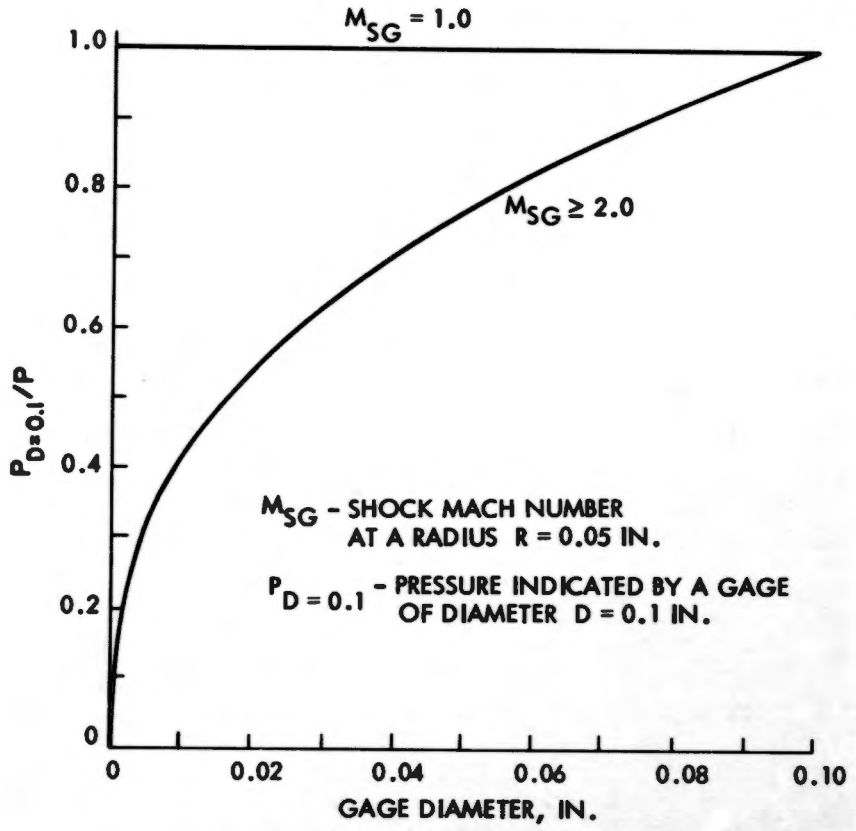

FIG. 11 INFLUENCE OF GAGE DIAMETER ON INDICATED PRESSURES

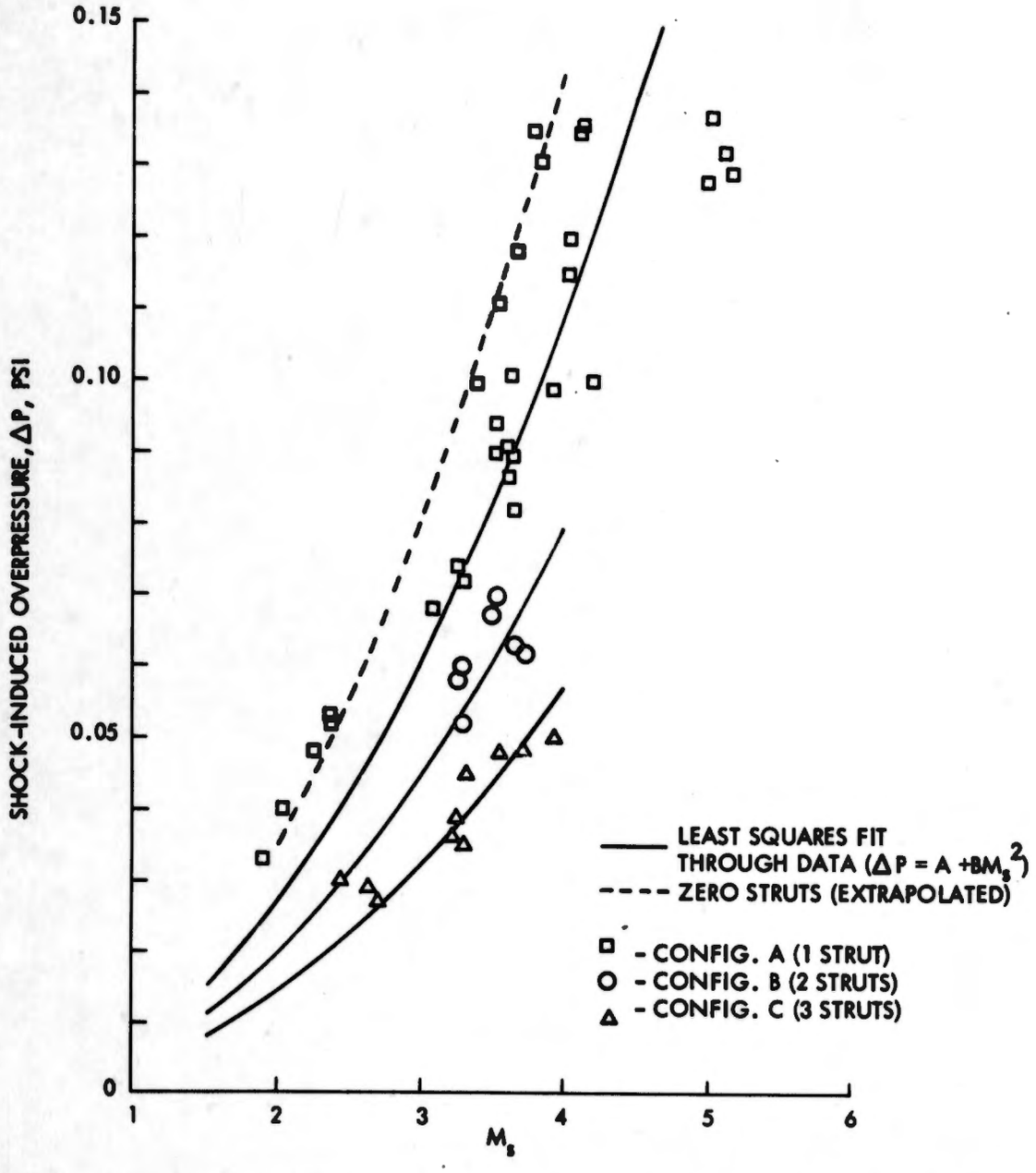

FIG. 12 PEAK OVERPRESSURE VERSUS BLAST WAVE INTENSITY FOR THREE SIDE STRUT CONFIGURATIONS; 9° SEMI-ANGLE CONE AT MACH NUMBER 5.1

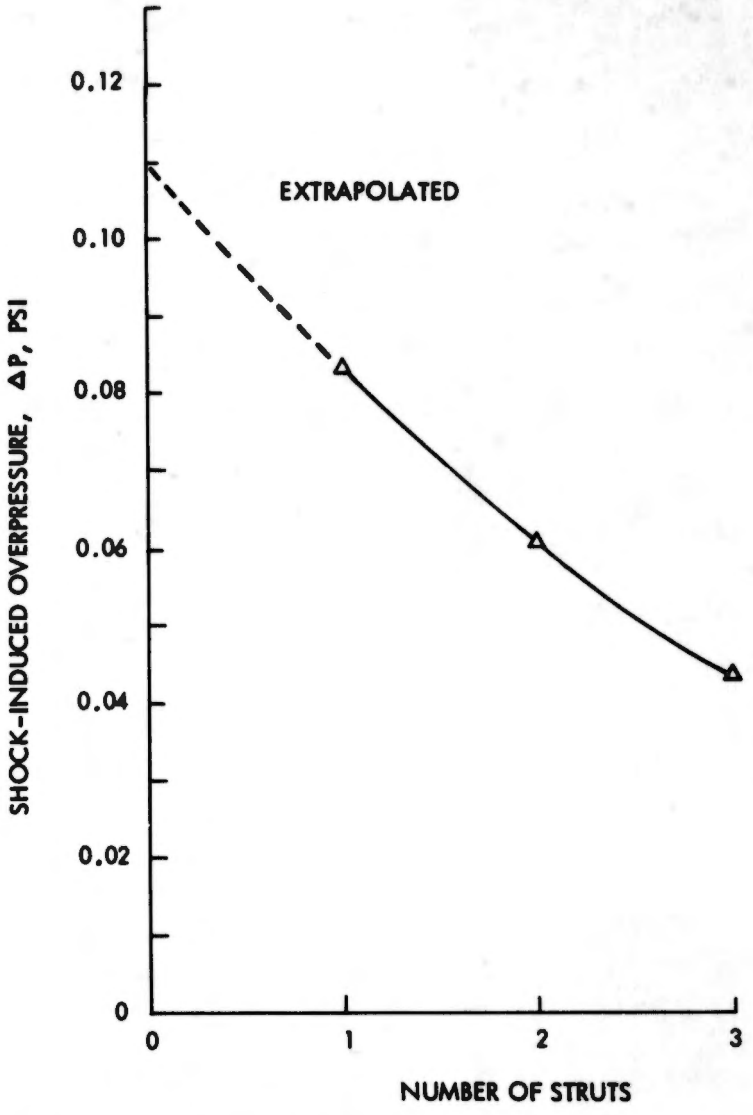

FIG. 13 PEAK OVERPRESSURE VERSUS NUMBER OF SIDE STRUTS FOR A 9° SEMI-ANGLE CONE AT A MACH NUMBER OF 5.1, AND A BLAST WAVE MACH NUMBER OF 3.5

A. $M_1 = 3.1$ $M_s = 2.8$

STA. 1 STA. 2 STA. 3

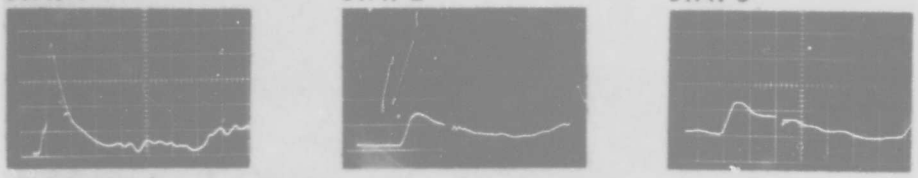

RUN 479

10 μ SEC/ cm ALL TRACES

B. $M_1 = 5.1$ $M_s = 5.3$

STA. 1 STA. 2 STA. 3

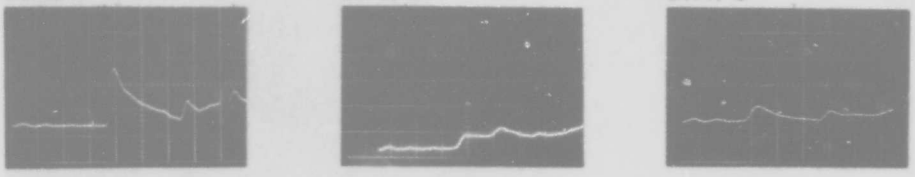

569

10 μ SEC/cm ALL TRACES

C. $M_1 = 6.5$ $M_s = 7.9$

STA. 1 STA. 2 STA. 3

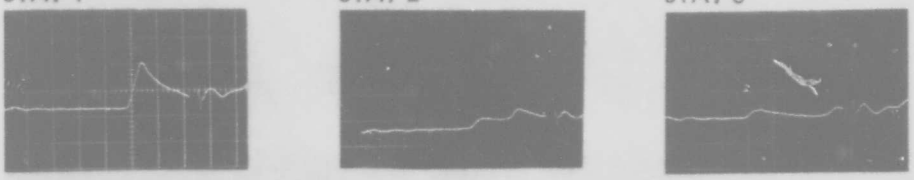

574

10 μ SEC/cm ALL TRACES

FIG. 14 POLAROID PICTURES OF TYPICAL PRESSURE-TIME TRACES

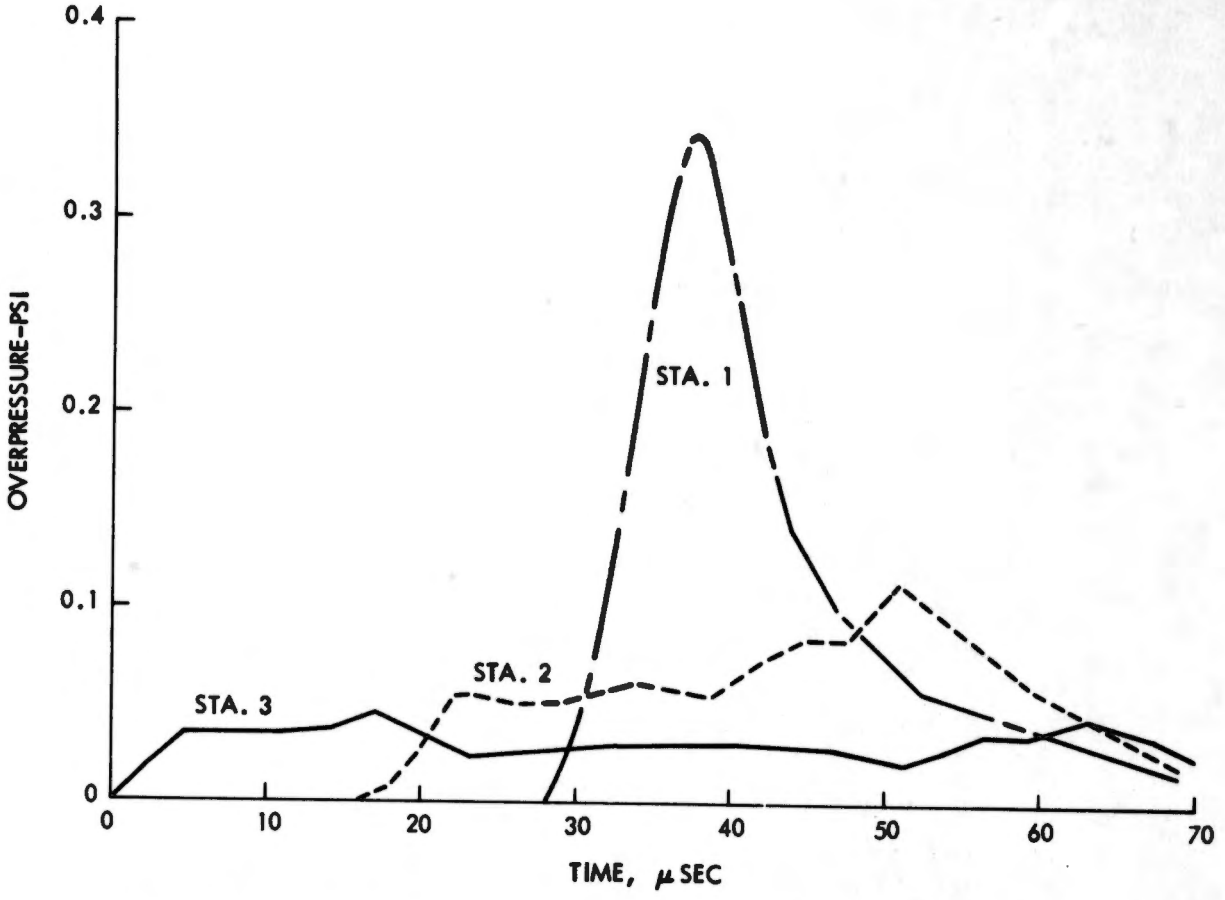

FIG. 15 PRESSURE-TIME VARIATIONS AT DIFFERENT DISTANCES FROM THE BASE CENTER
A. $M_1 = 3.1$
$M_s = 1.49$ (RUN 553)

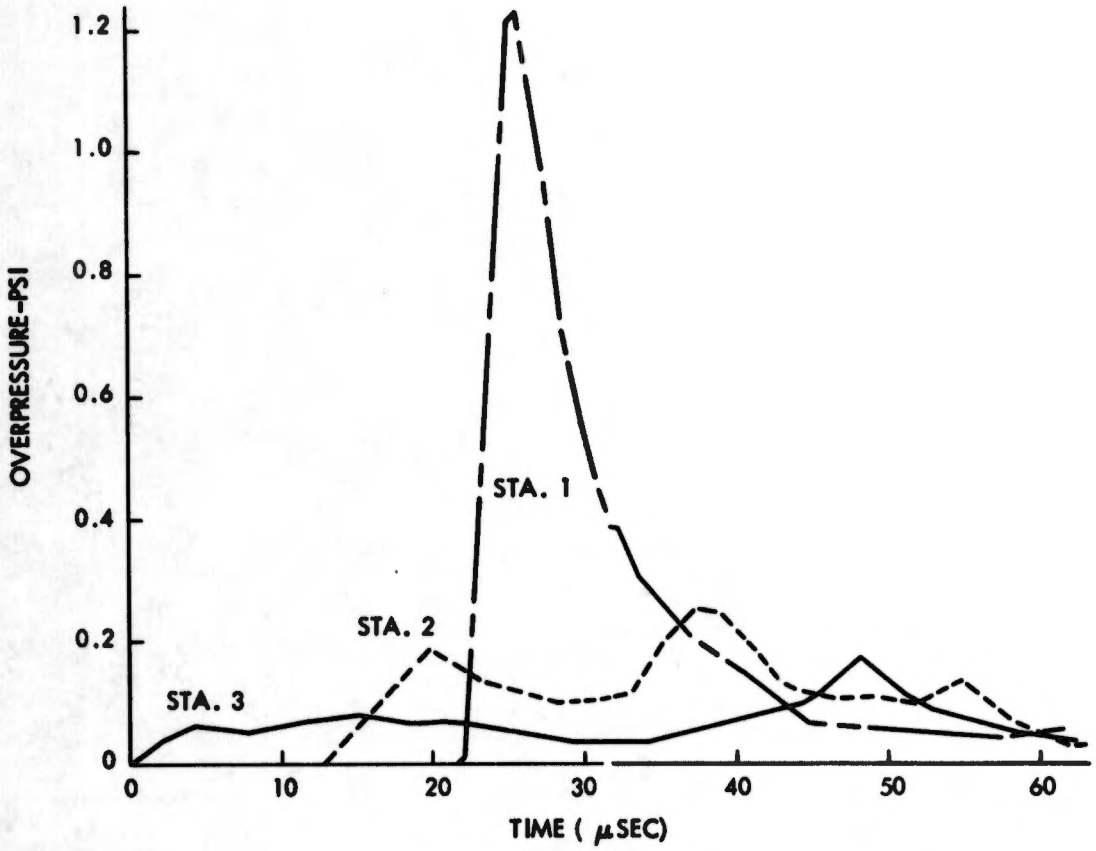

FIG. 15 (CONTINUED)
B. $M_1 = 3.1$
$M_s = 2.36$ (RUN 543)

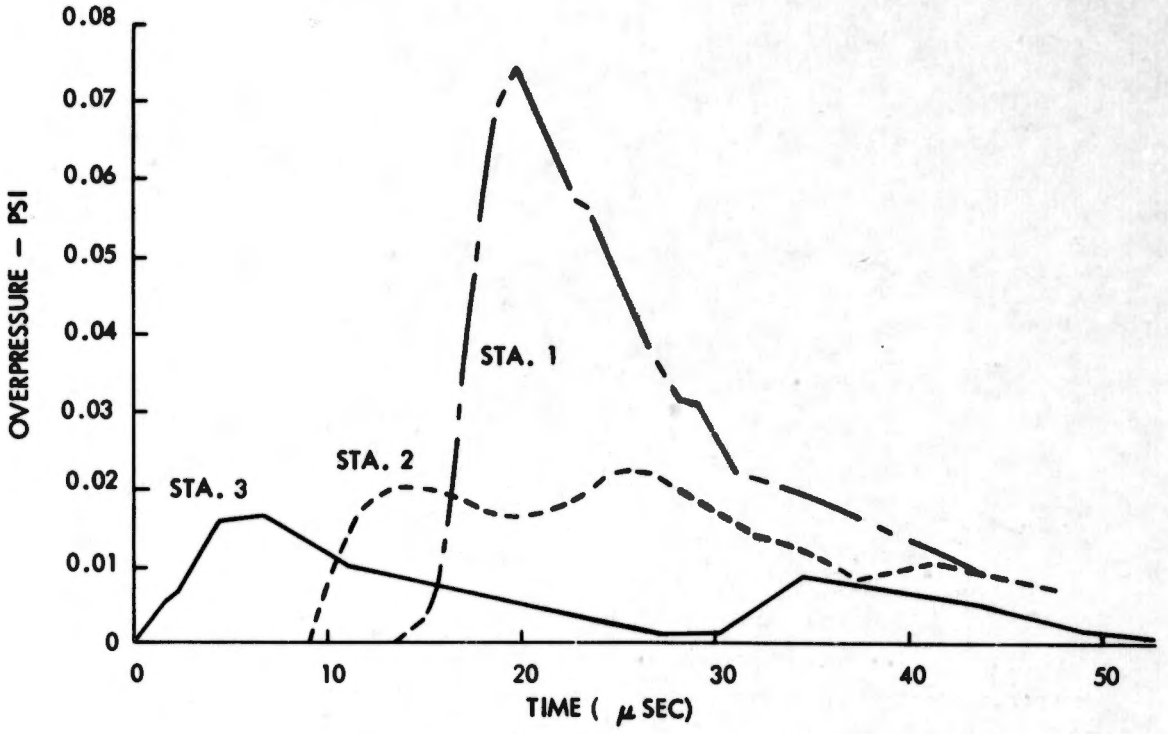

FIG. 15 (CONTINUED)
C. $M_1 = 5.1$
$M_s = 3.05$ (RUN 560)

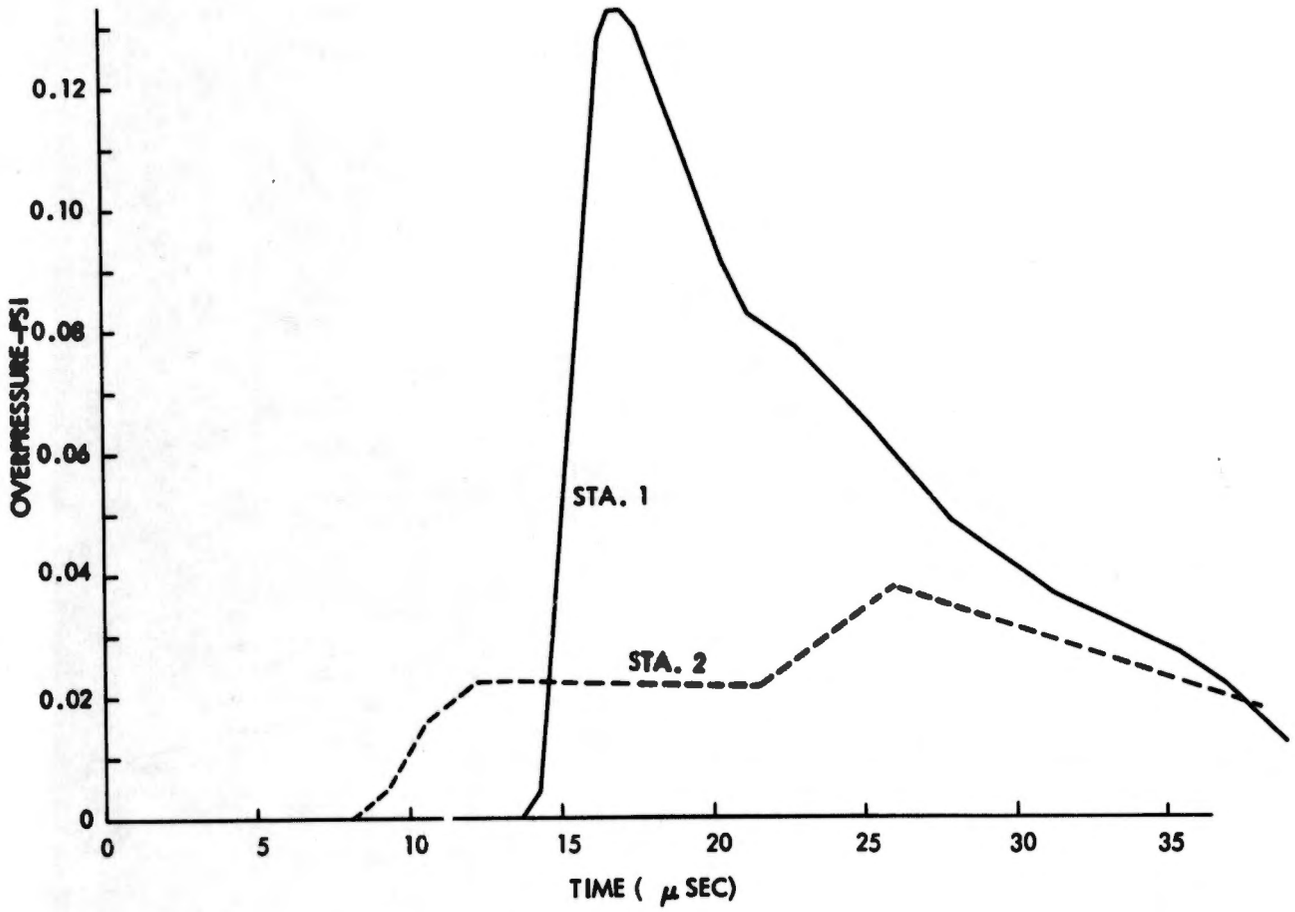

FIG. 15 (CONTINUED)
D. $M_1 = 5.1$
$M_s = 5.25$ (RUN 568)

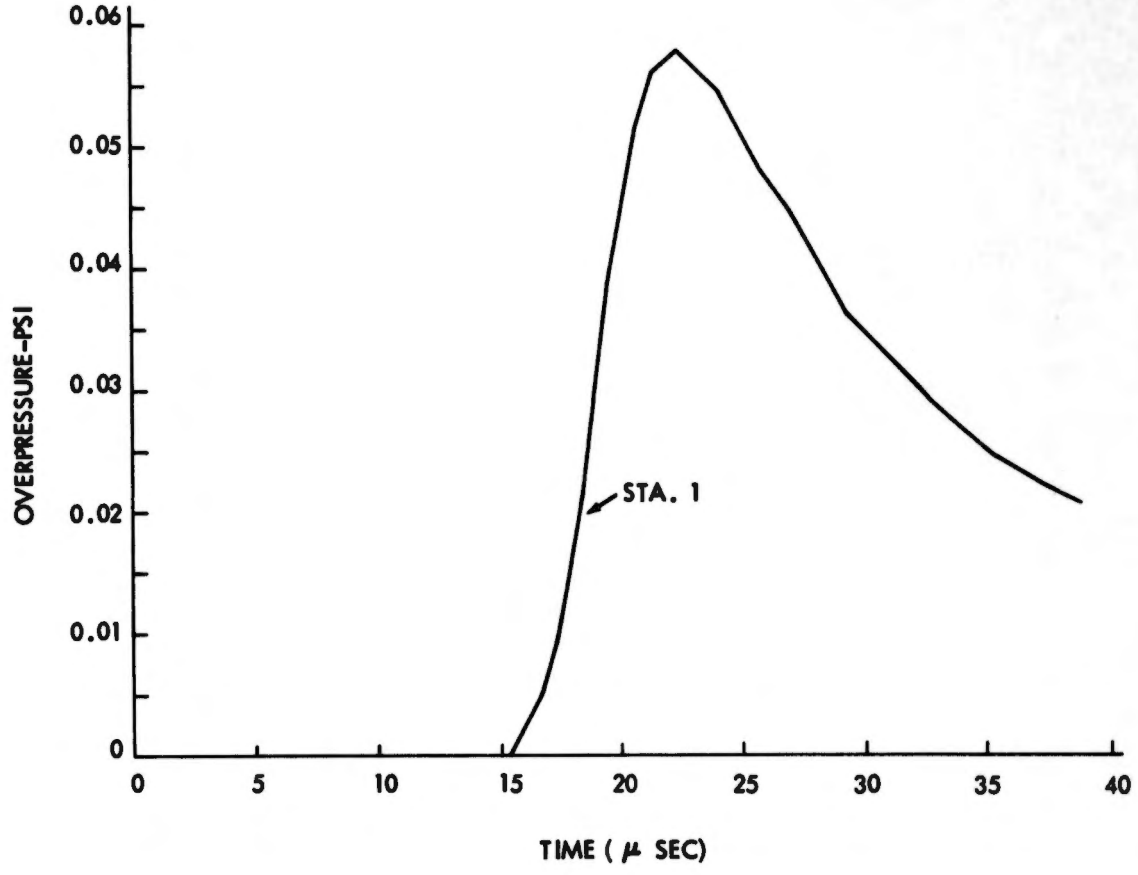

FIG. 15 (CONTINUED)
E. $M_1 = 6.5$
$M_s = 7.48$ (RUN 580)

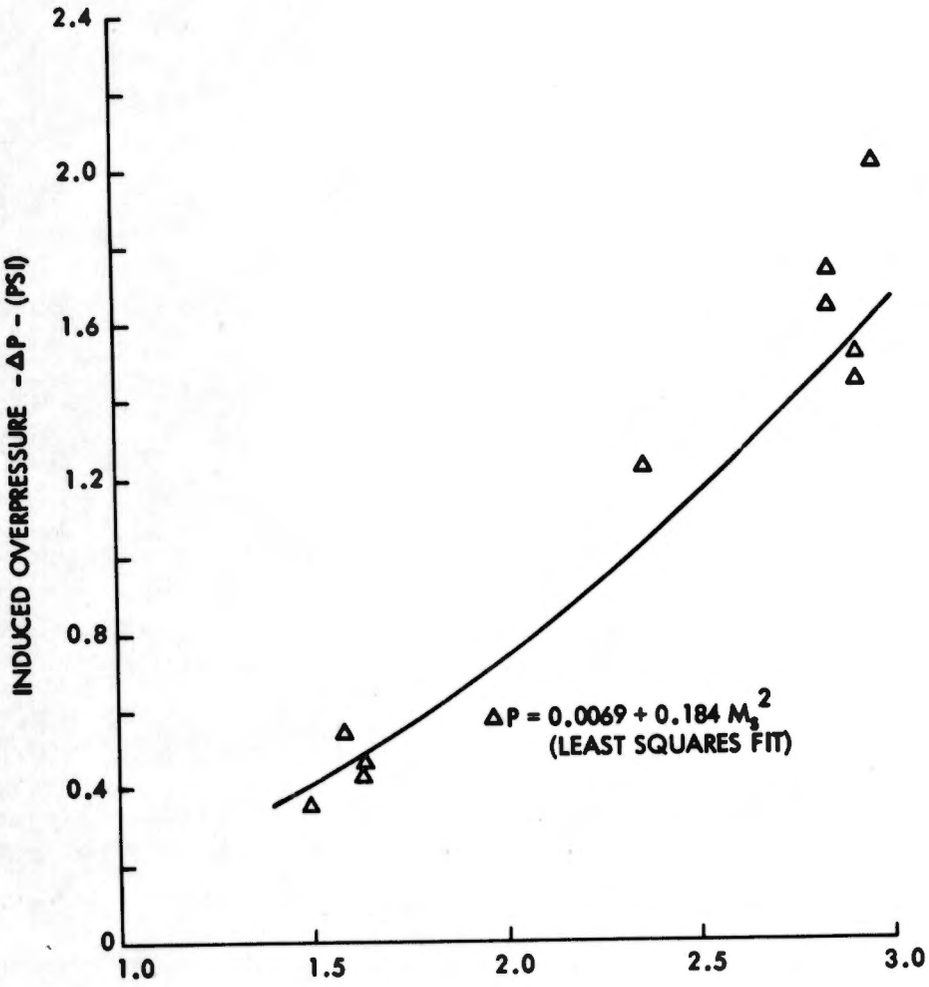

FIG. 16 INDUCED OVERPRESSURE VS. BLAST WAVE INTENSITY
A. $M_1 = 3.1$

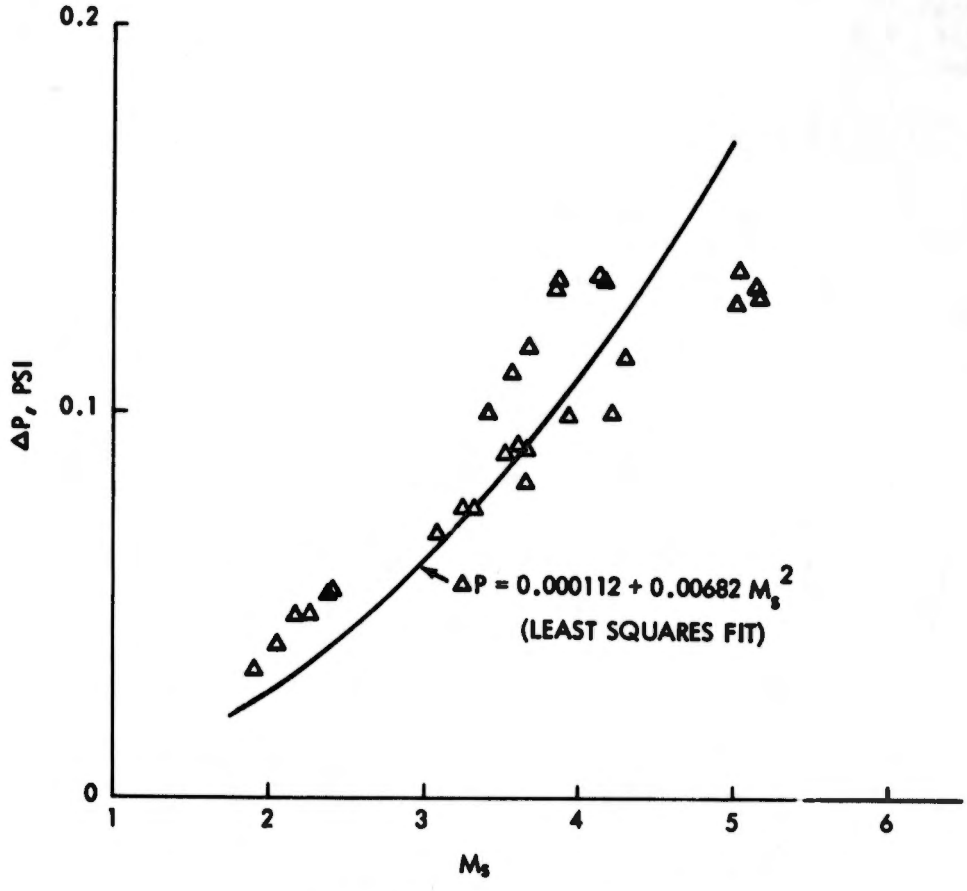

FIG. 16 (CONTINUED)
B. $M_1 = 5.1$

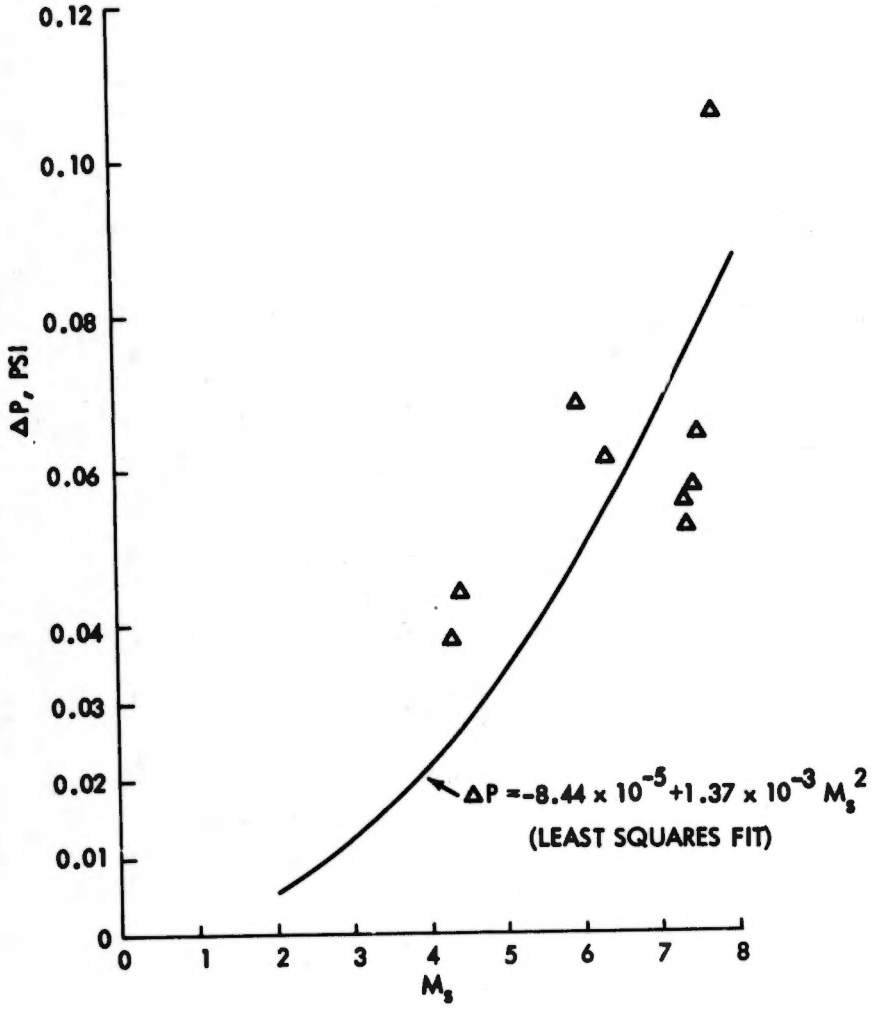

FIG. 16 (CONTINUED)
C. $M_1 = 6.5$

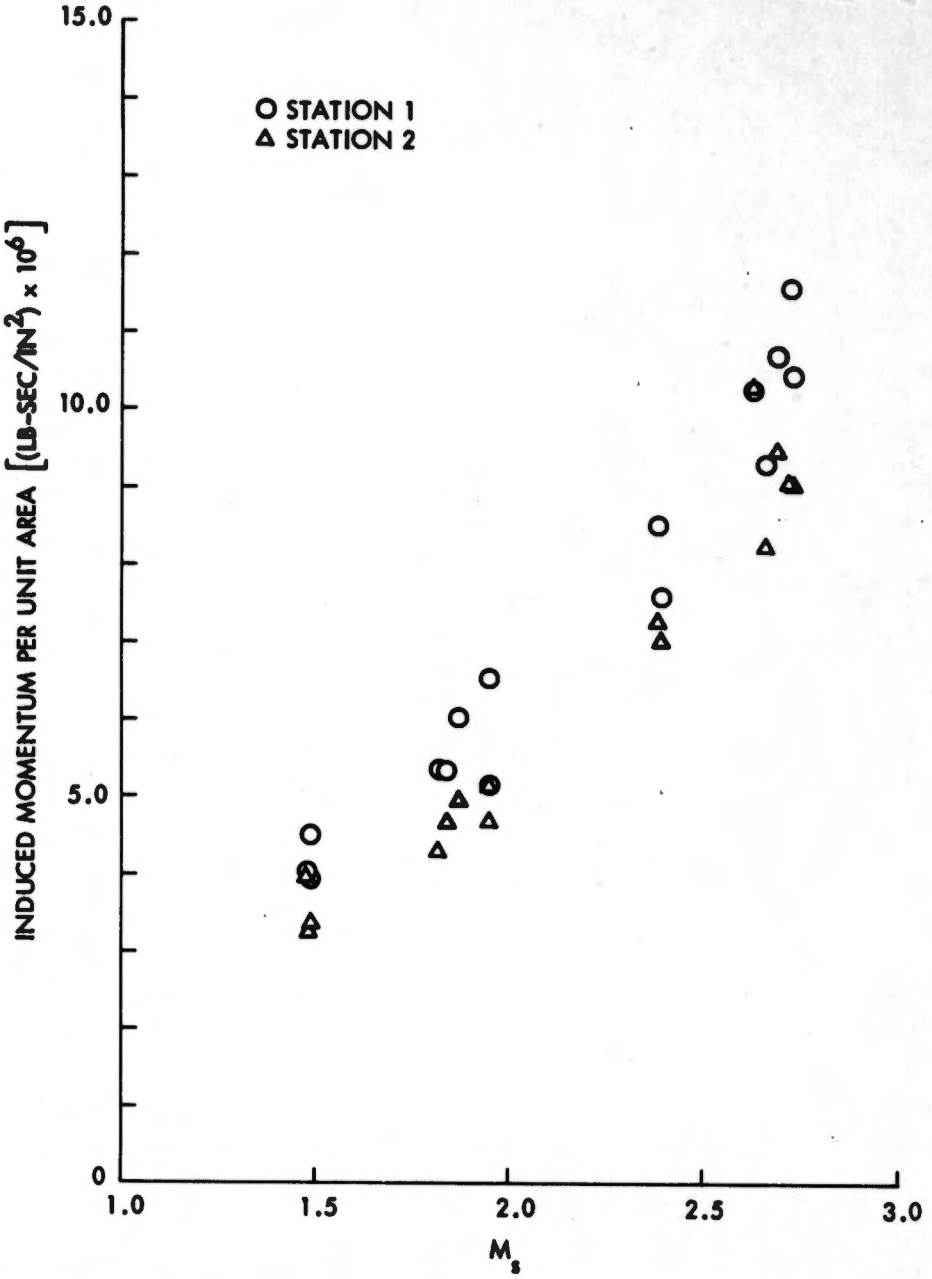

FIG. 17 SHOCK-INDUCED MOMENTUM VERSUS SHOCK MACH NUMBER AT $M_1 = 3.1$

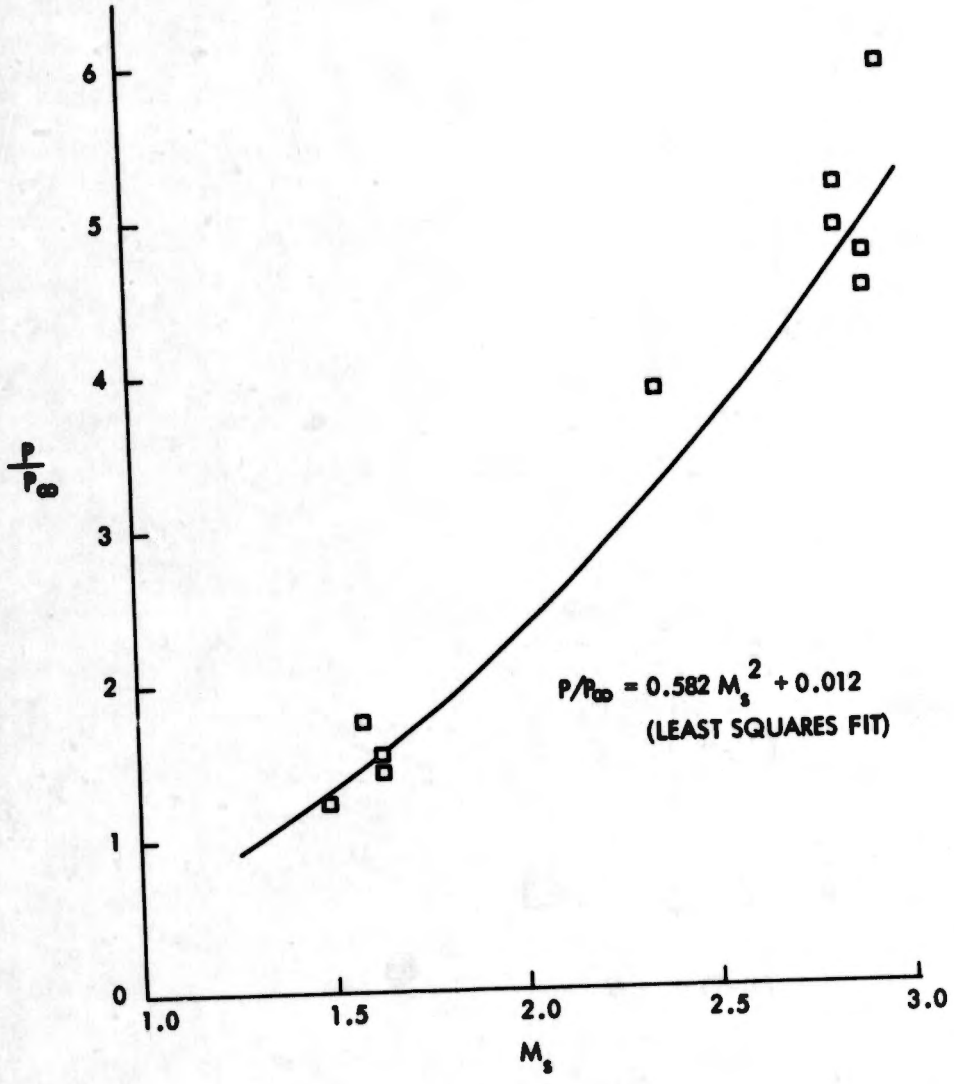

FIG. 18 RATIO OF SHOCK-INDUCED PRESSURE TO FREE-STREAM STATIC PRESSURE VS. BLAST WAVE INTENSITY
A. $M_1 = 3.1$

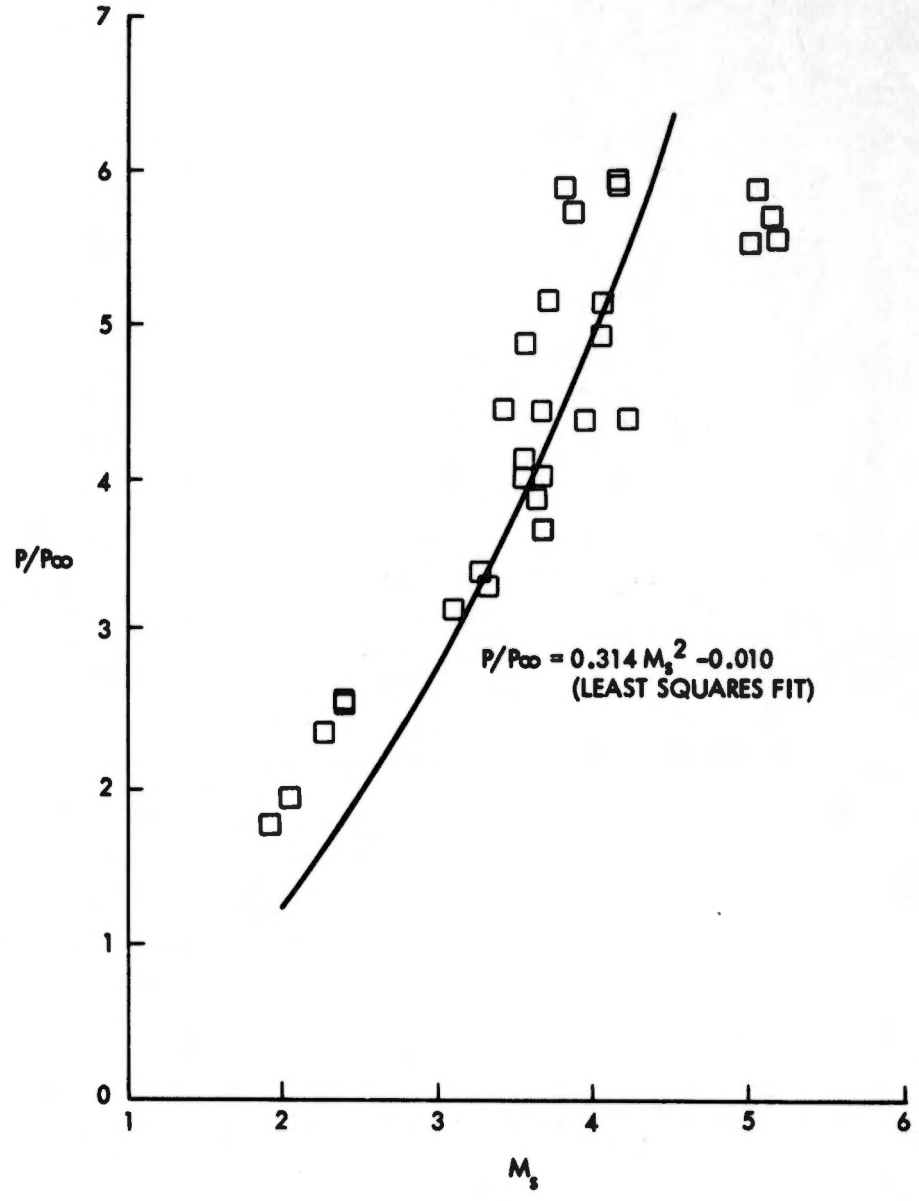

FIG. 18 (CONTINUED)
B. $M_1 = 5.1$

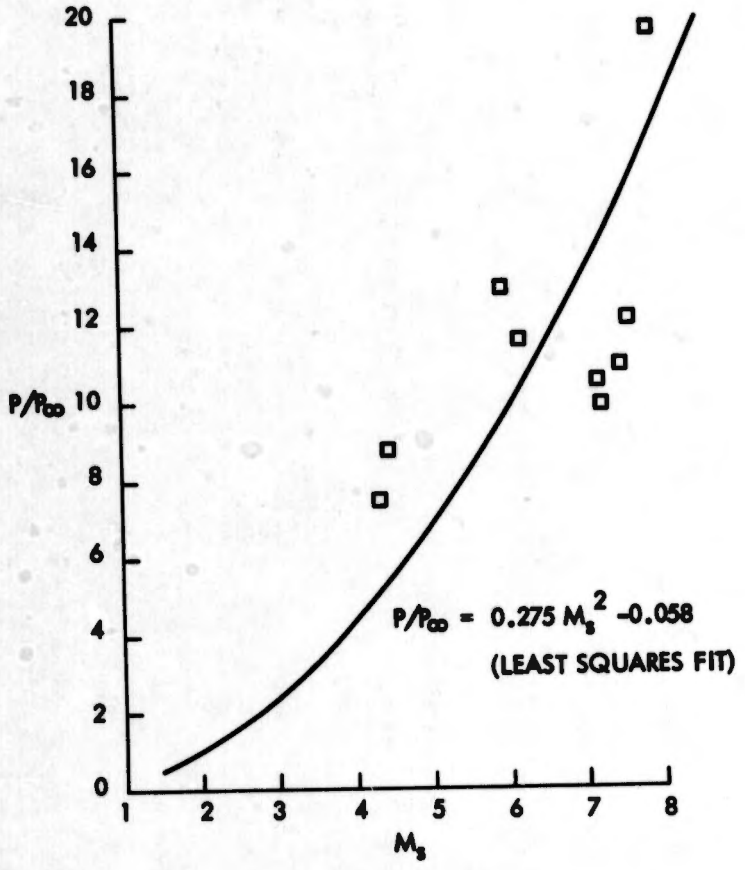

FIG. 18 (CONTINUED)
C. $M_1 = 6.5$

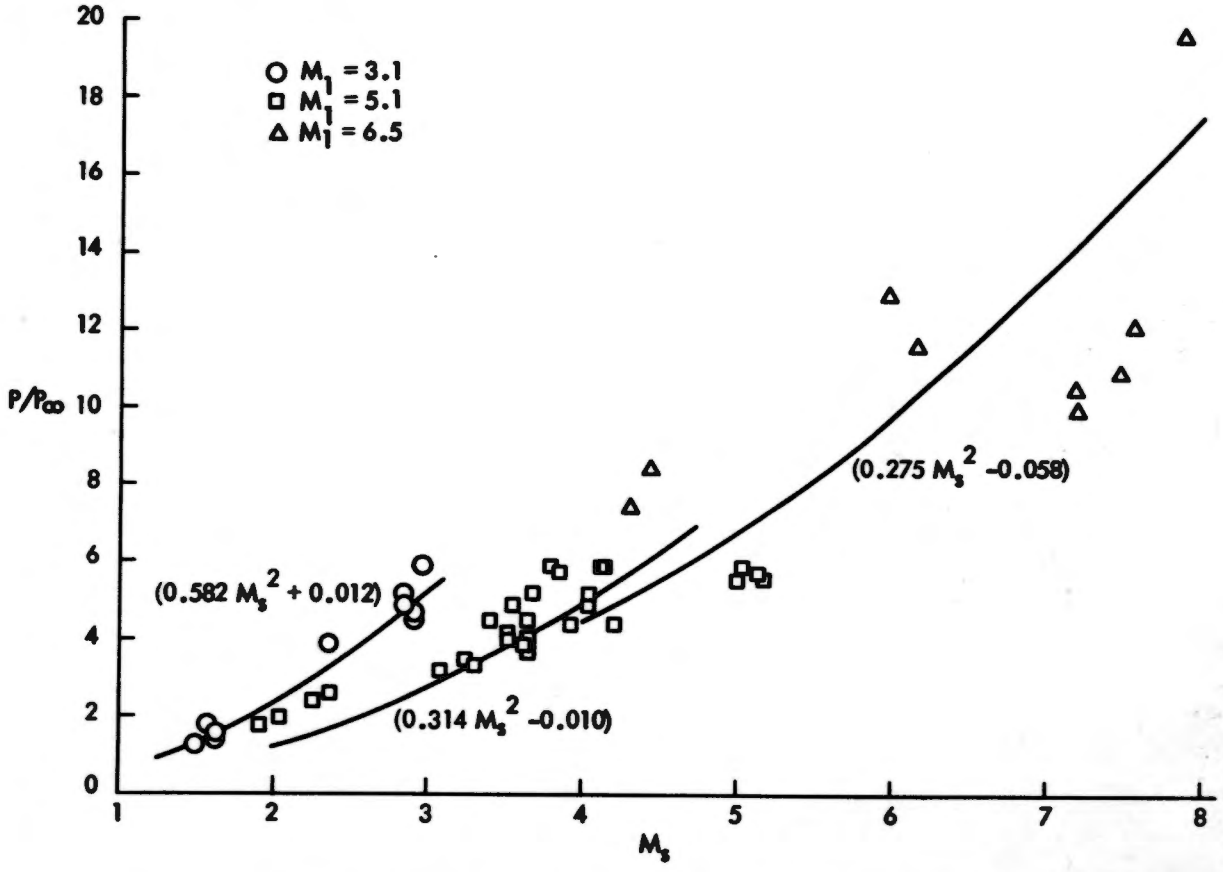

FIG. 19 RATIO OF SHOCK-INDUCED PRESSURE TO FREE-STREAM STATIC PRESSURE VS. BLAST WAVE INTENSITY AT M_1 = 3.1, 5.1 AND 6.5

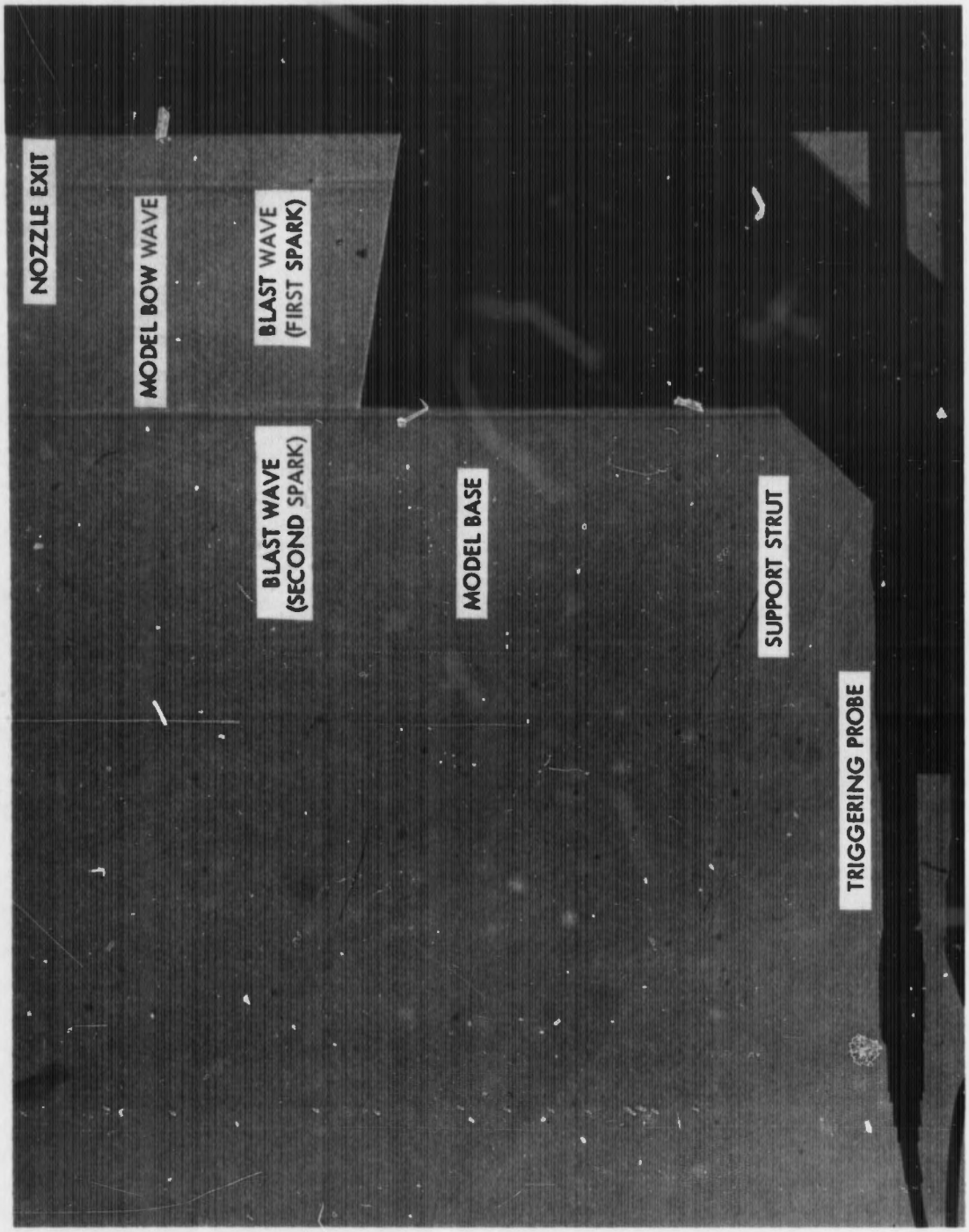

FIG. 20 TWO-SPARK SHADOWGRAPH
A. $M_1 = 3.1$, $M_s = 1.49$

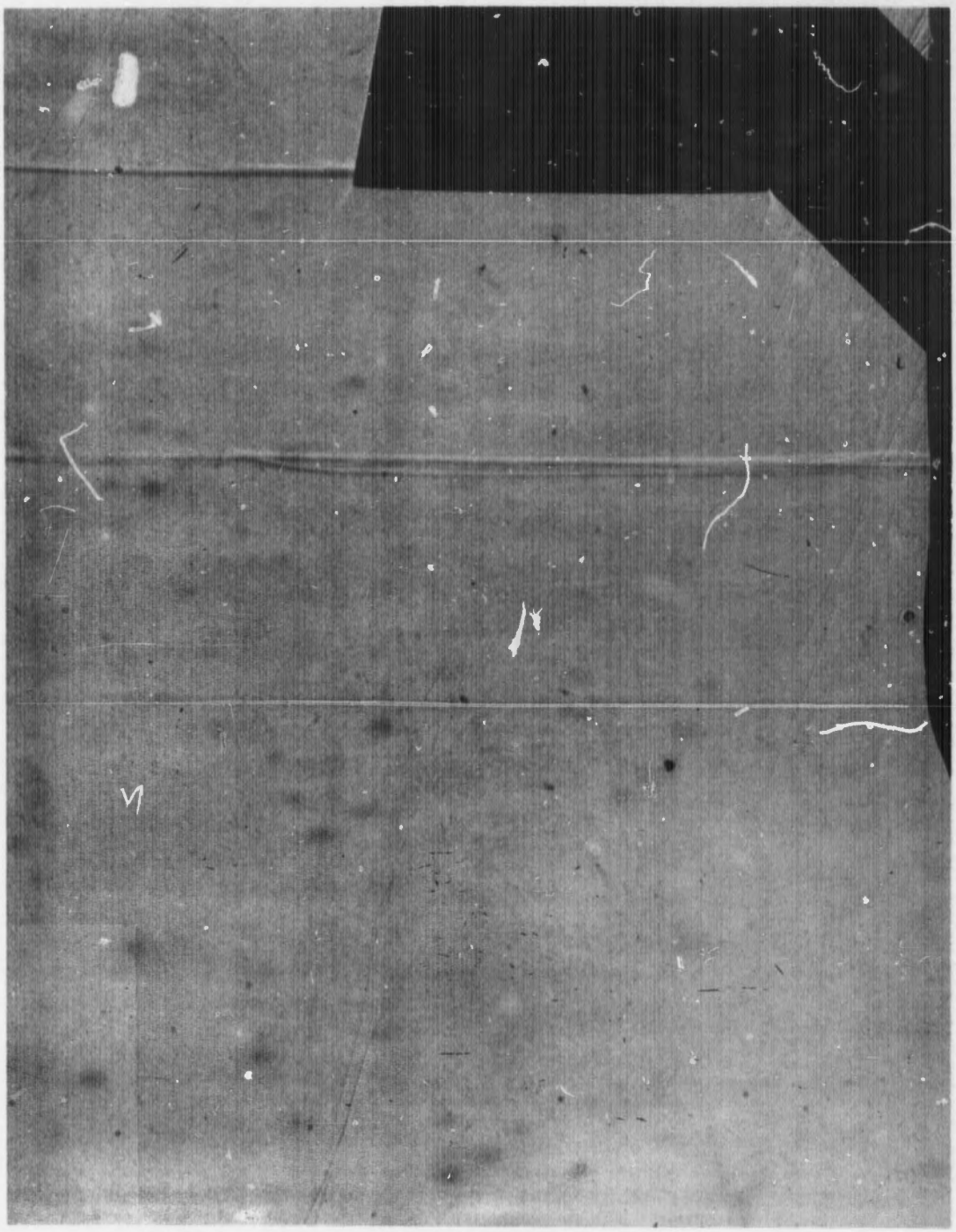

FIG. 20 CONT.
B. $M_1 = 3.1, M_s = 1.58$

FIG. 20 CONT.
C. $M_1 = 3.1$, $M_s = 1.63$

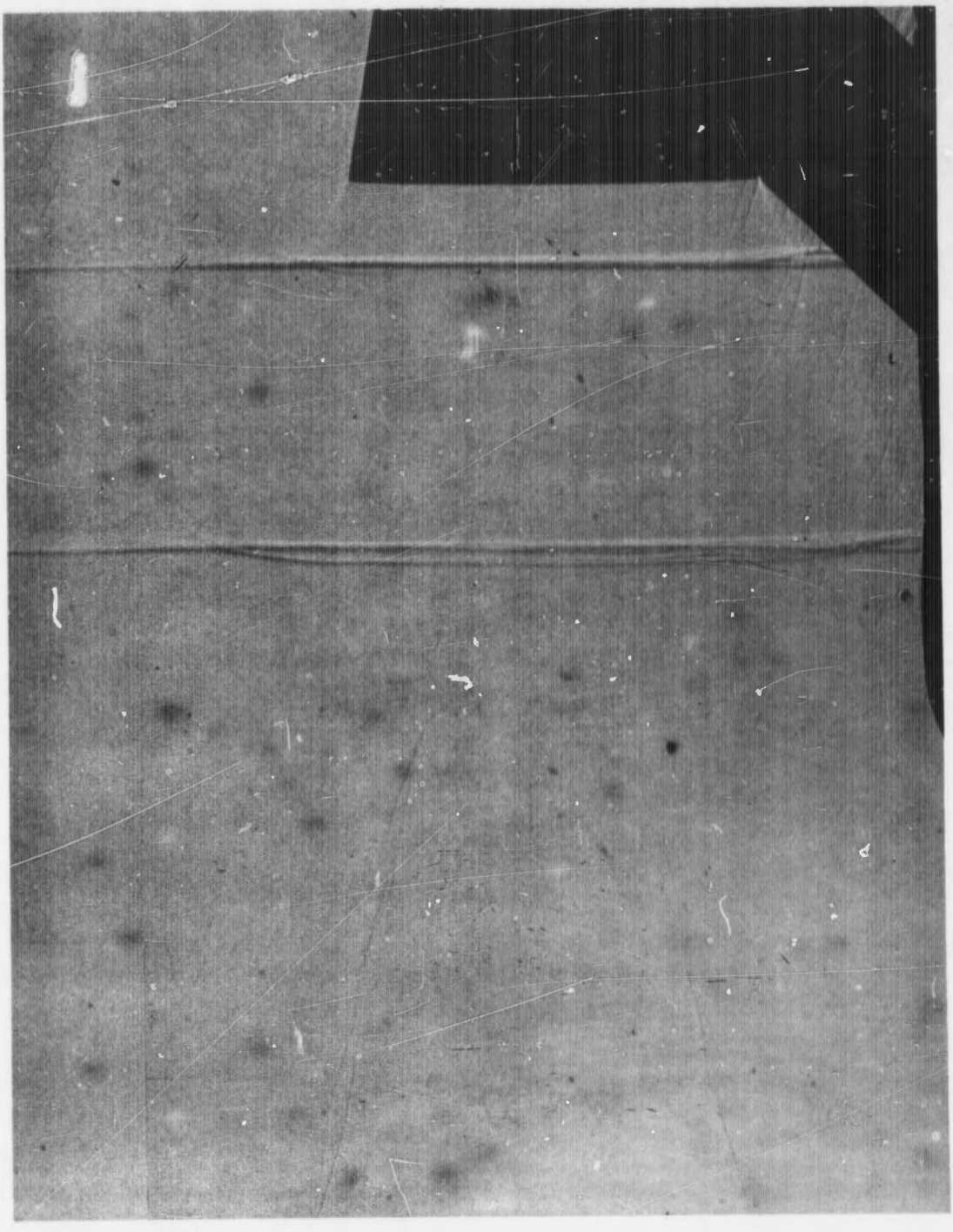

FIG. 20 CONT.
D. $M_1 = 3.1$, $M_s = 1.63$

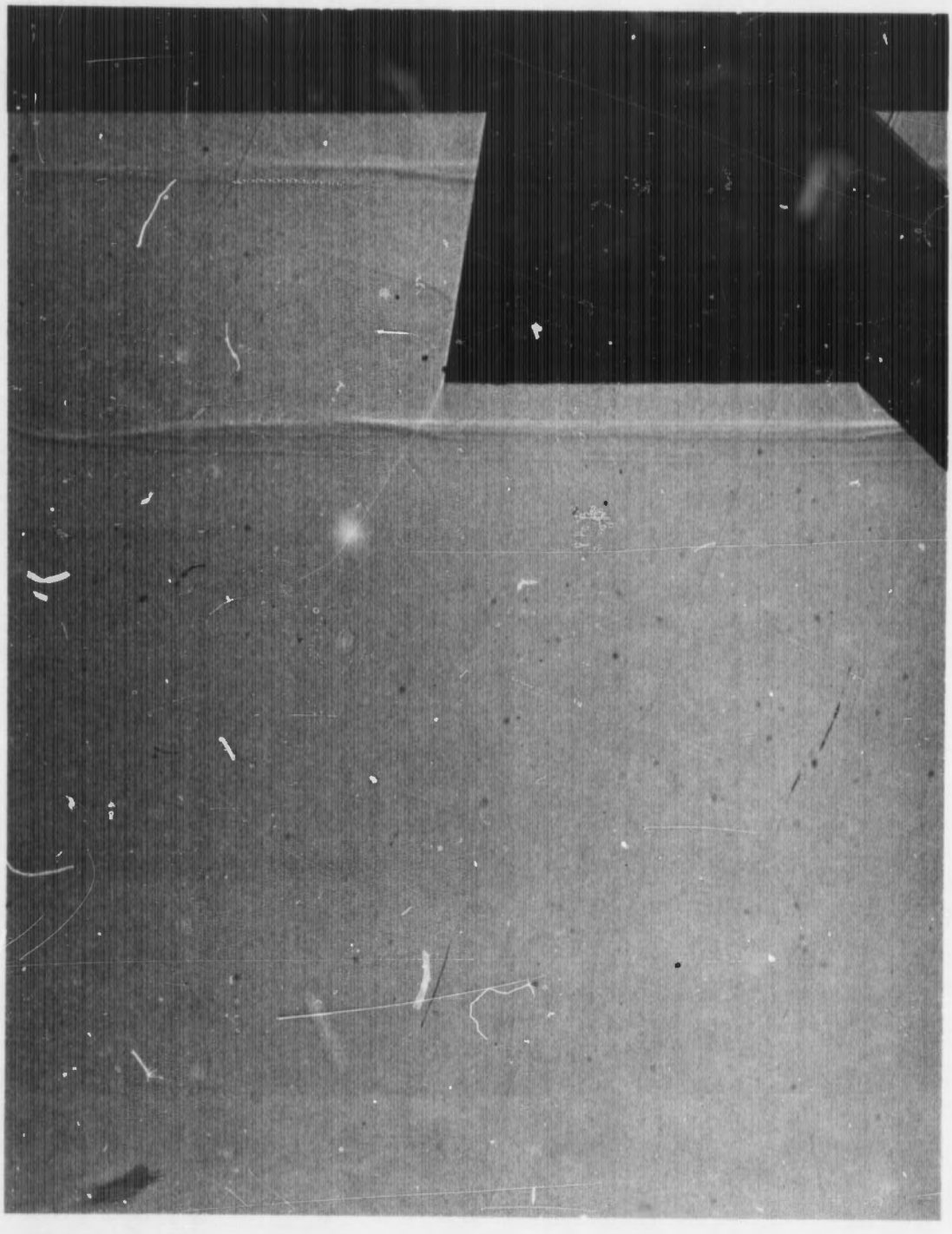

FIG. 20 CONT.
E. $M_1 = 3.1$, $M_s = 2.36$

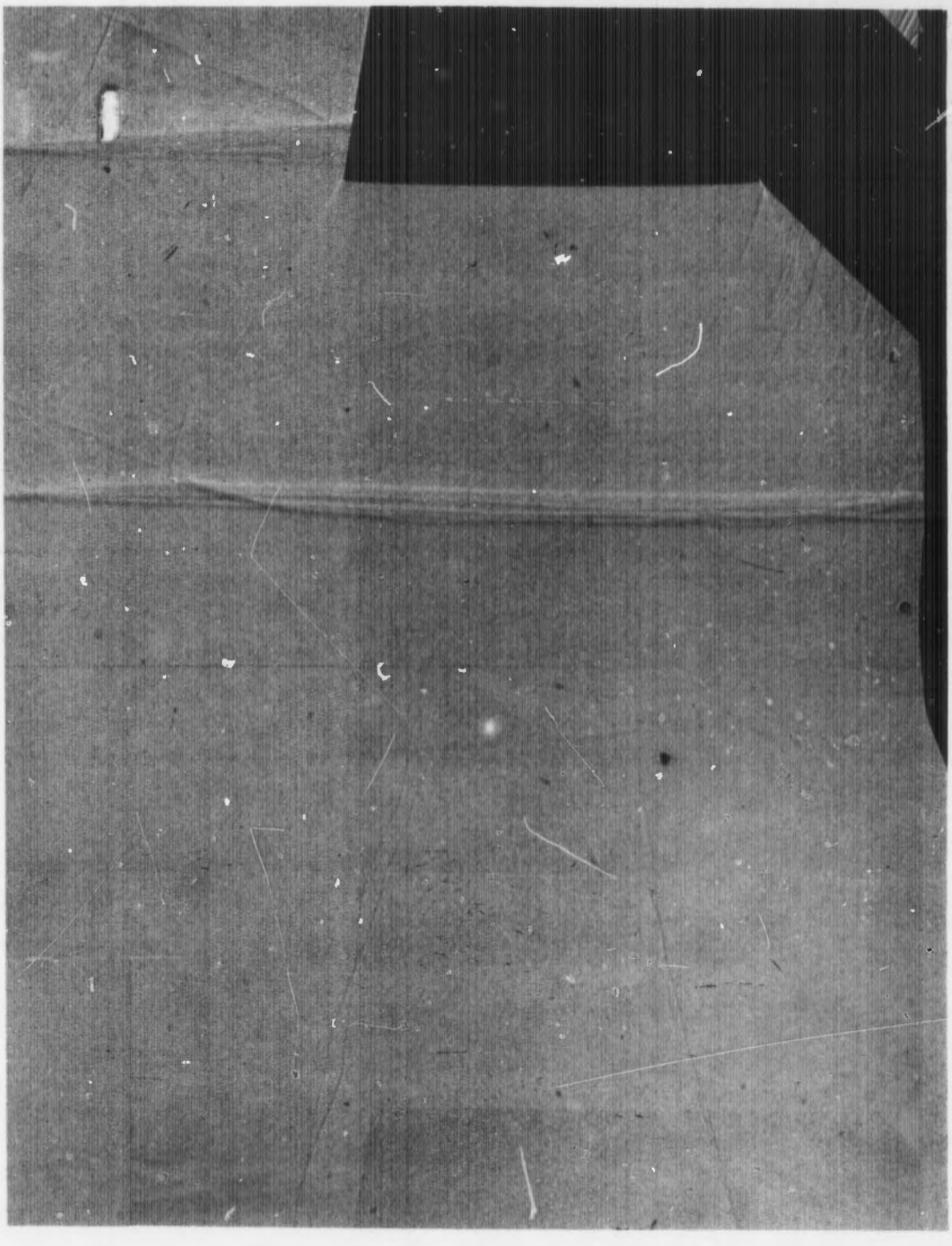

FIG. 20 CONT.
F. $M_1 = 3.1$, $M_s = 2.84$

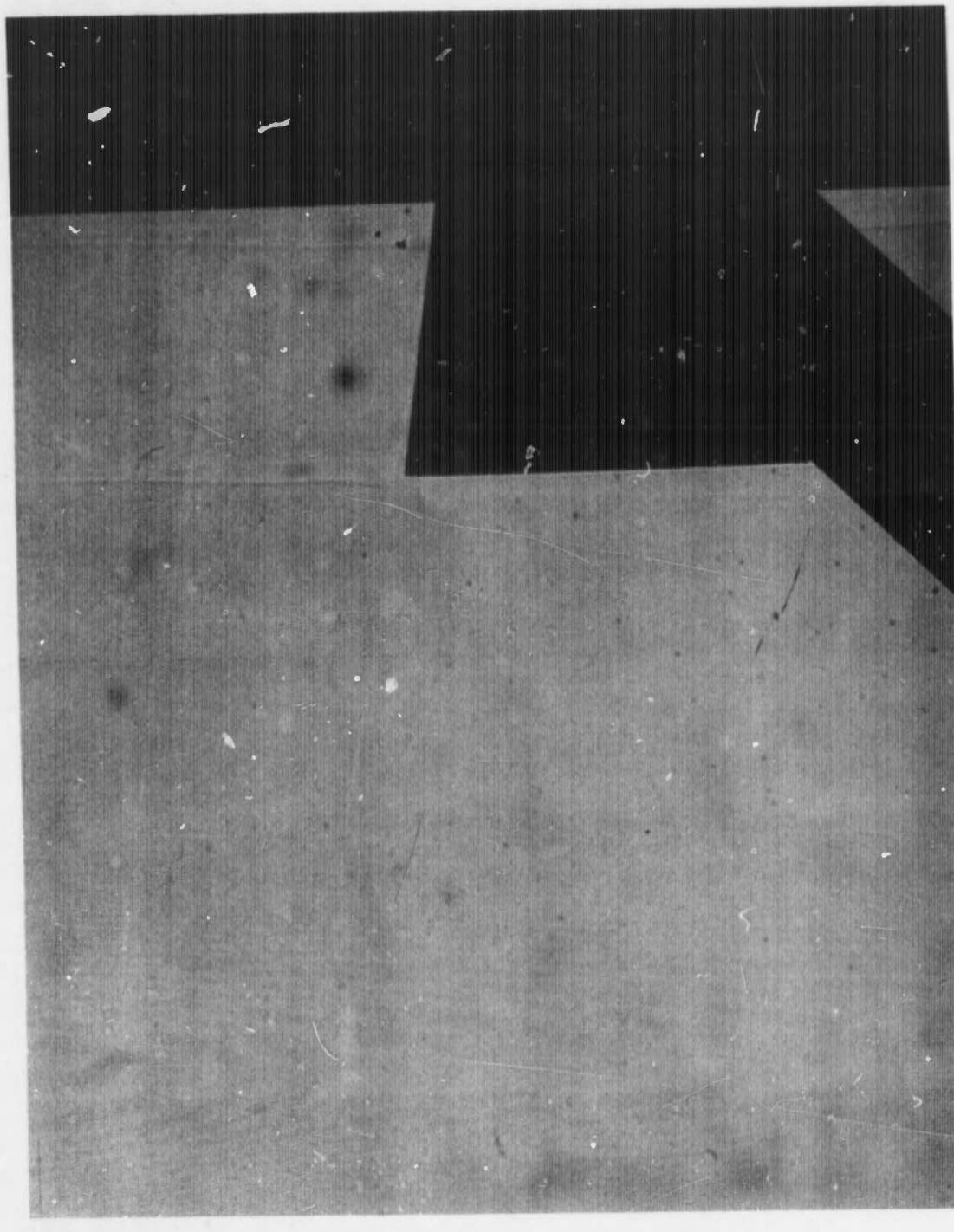

FIG. 20 CONT.
G. $M_1 = 5.1$, $M_s = 1.90$

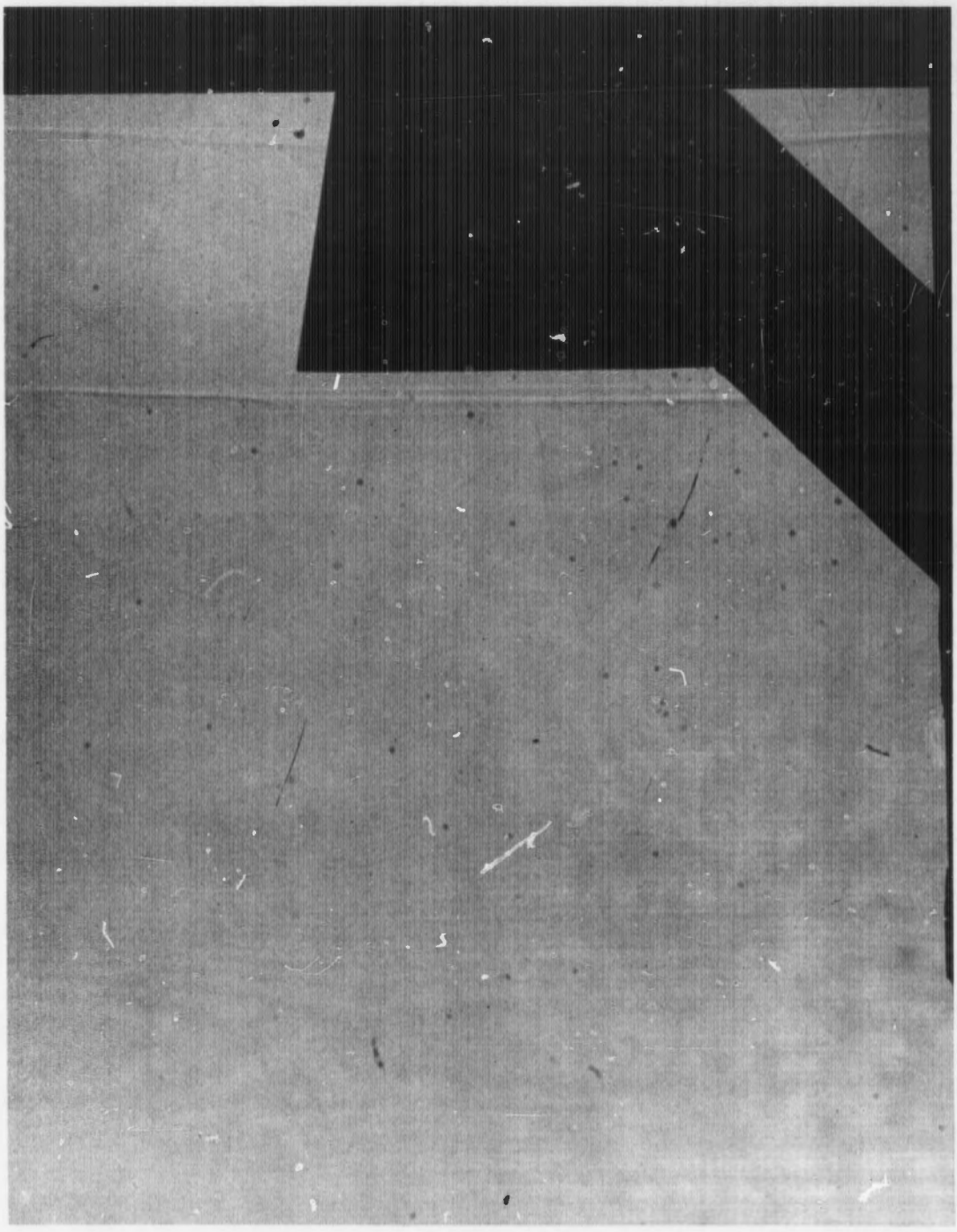

FIG. 20 CONT.
H. $M_1 = 5.1$, $M_s = 2.37$

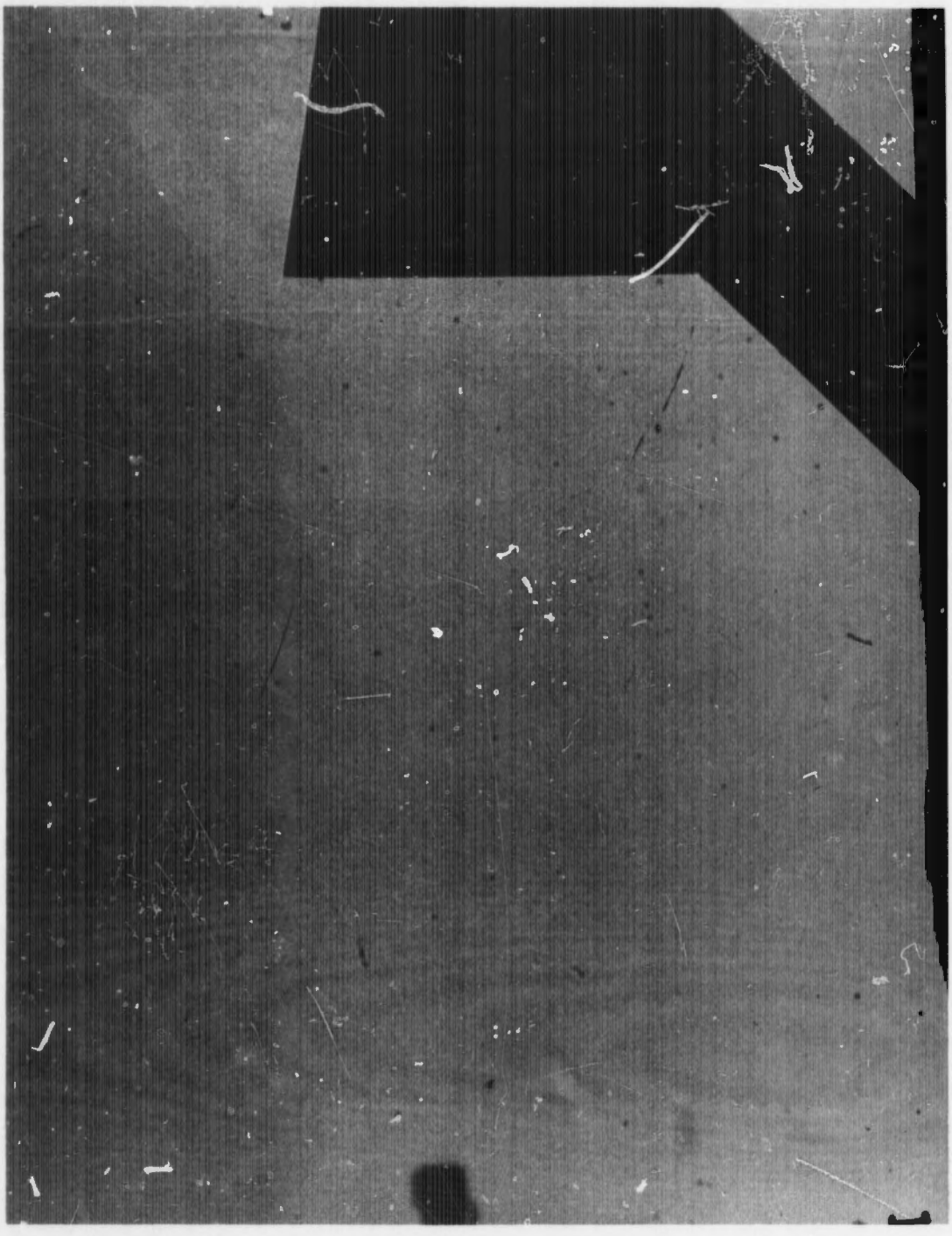

FIG. 20 CONT.
I. $M_1 = 5.1$, $M_s = 3.08$

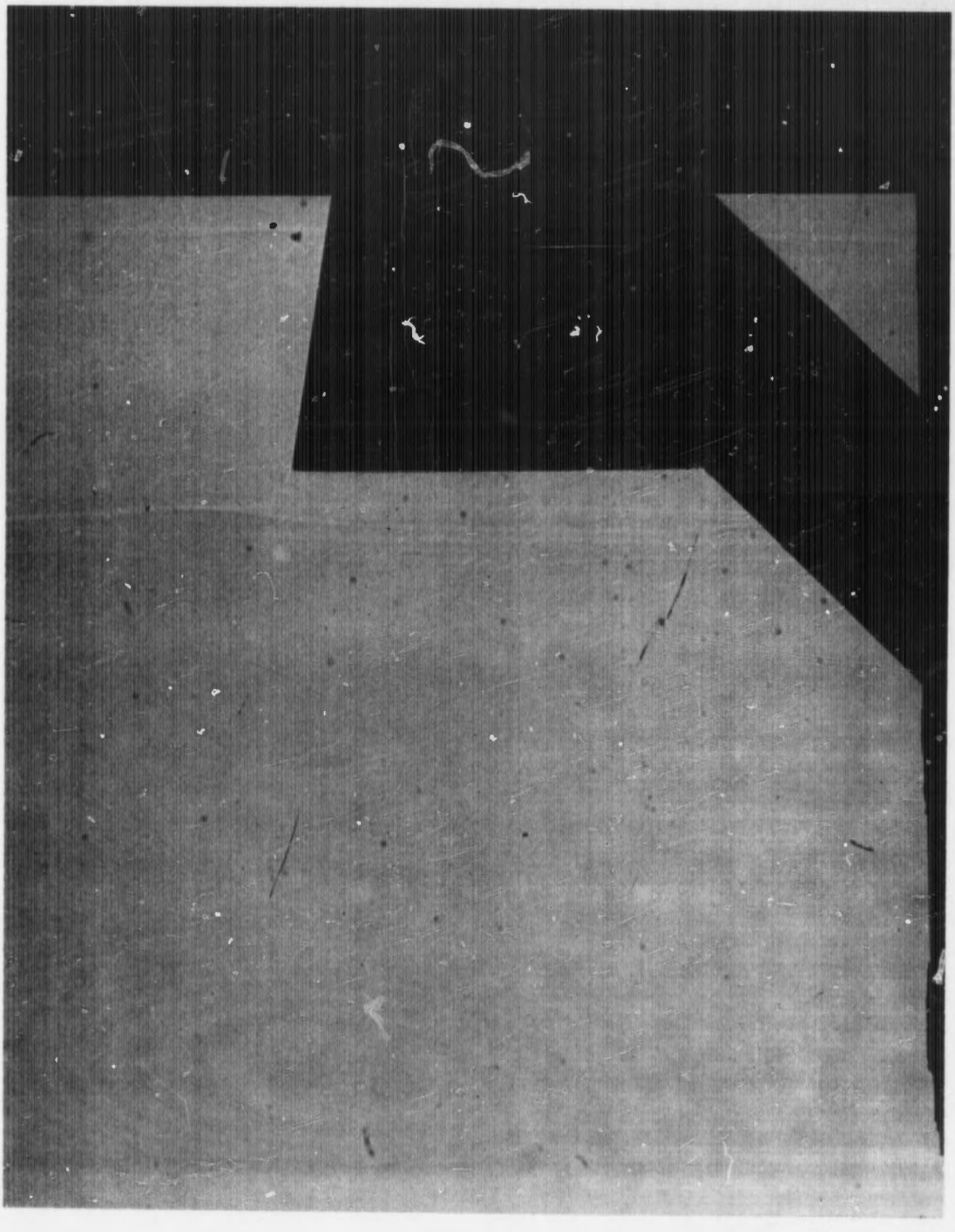

FIG. 20 CONT.
J. $M_1 = 5.1, M_s = 3.25$

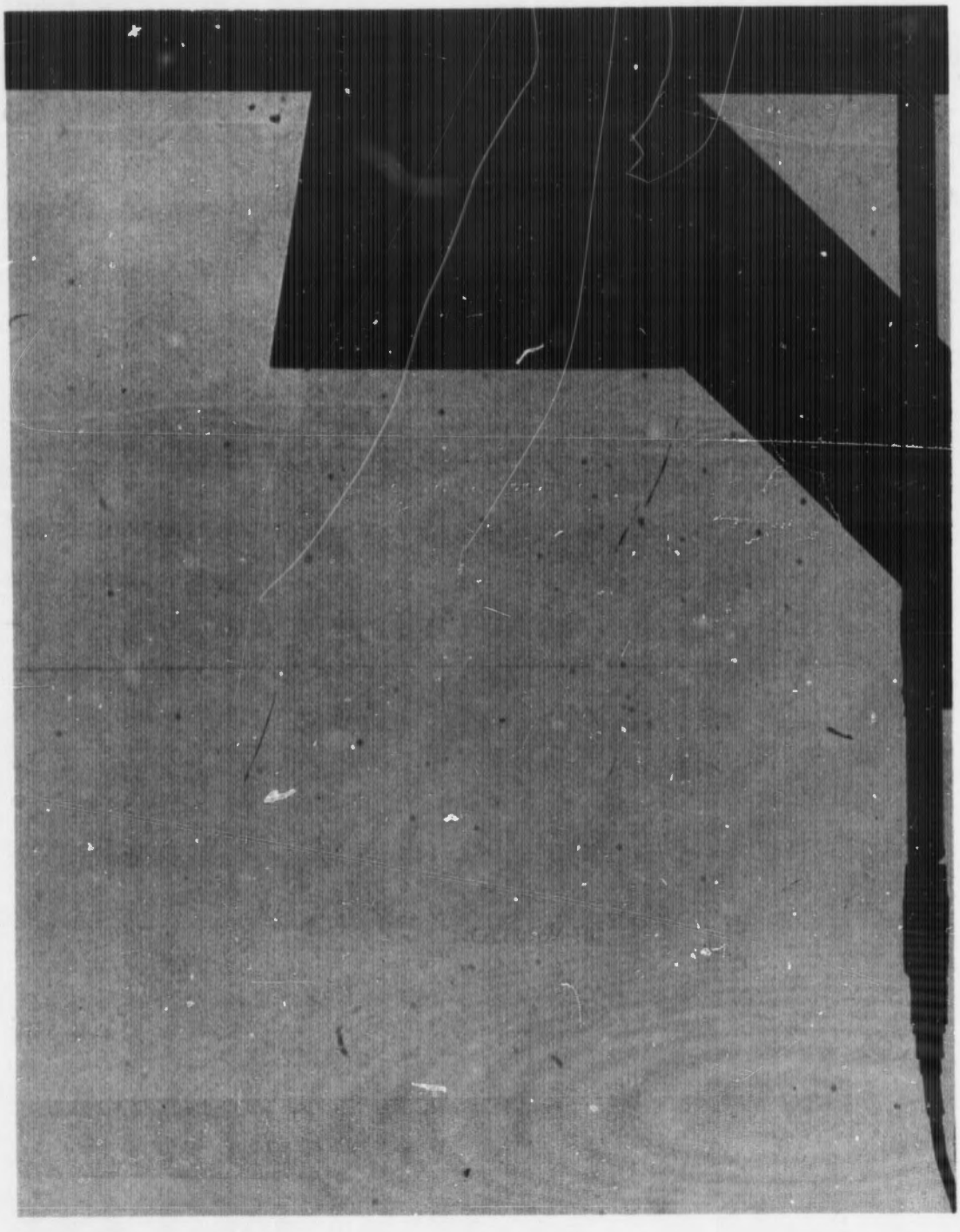

FIG. 20 CONT.
K. $M_1 = 5.1$, $M_s = 3.30$

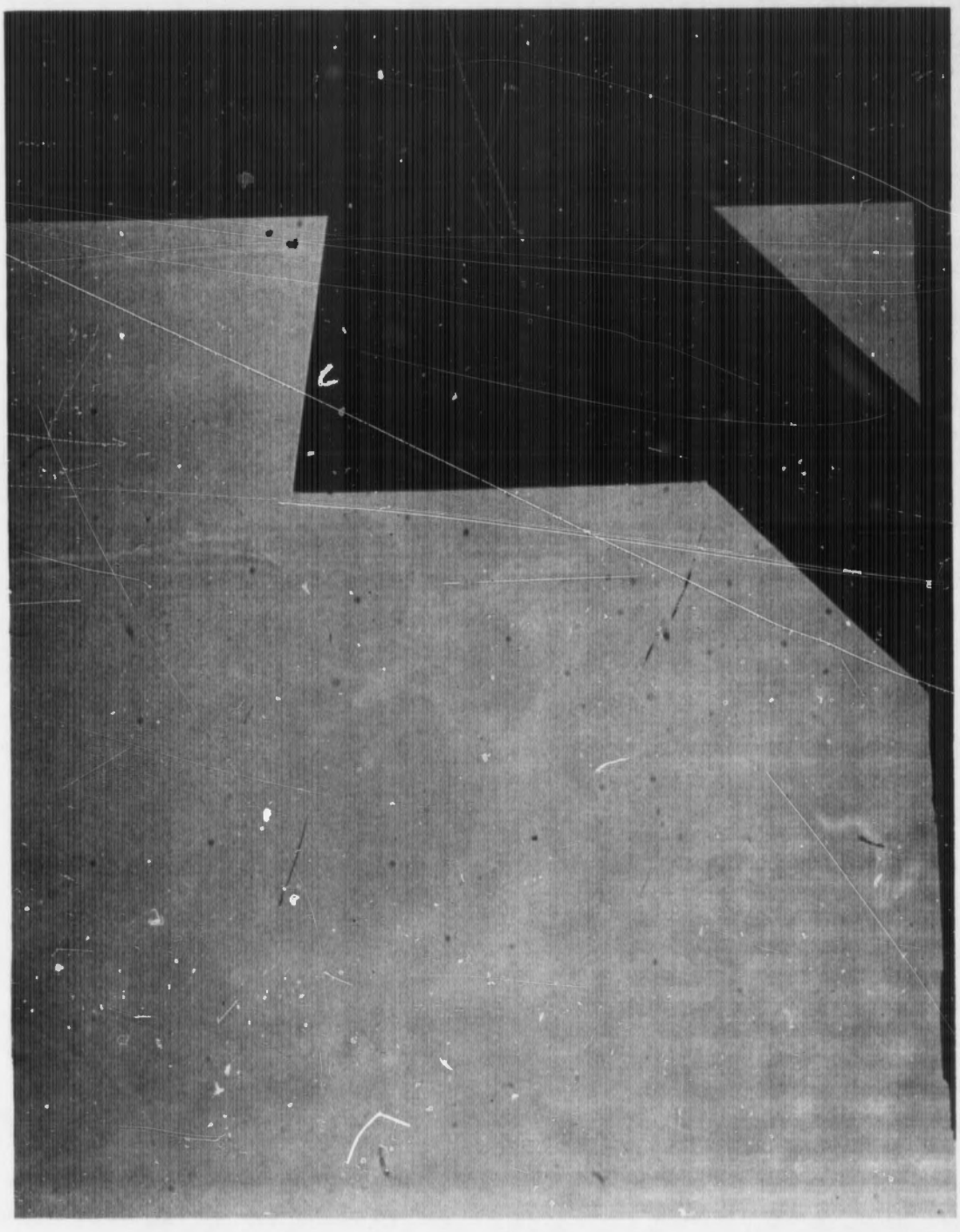

FIG. 20 CONT.
L. $M_1 = 5.1$, $M_s = 3.52$

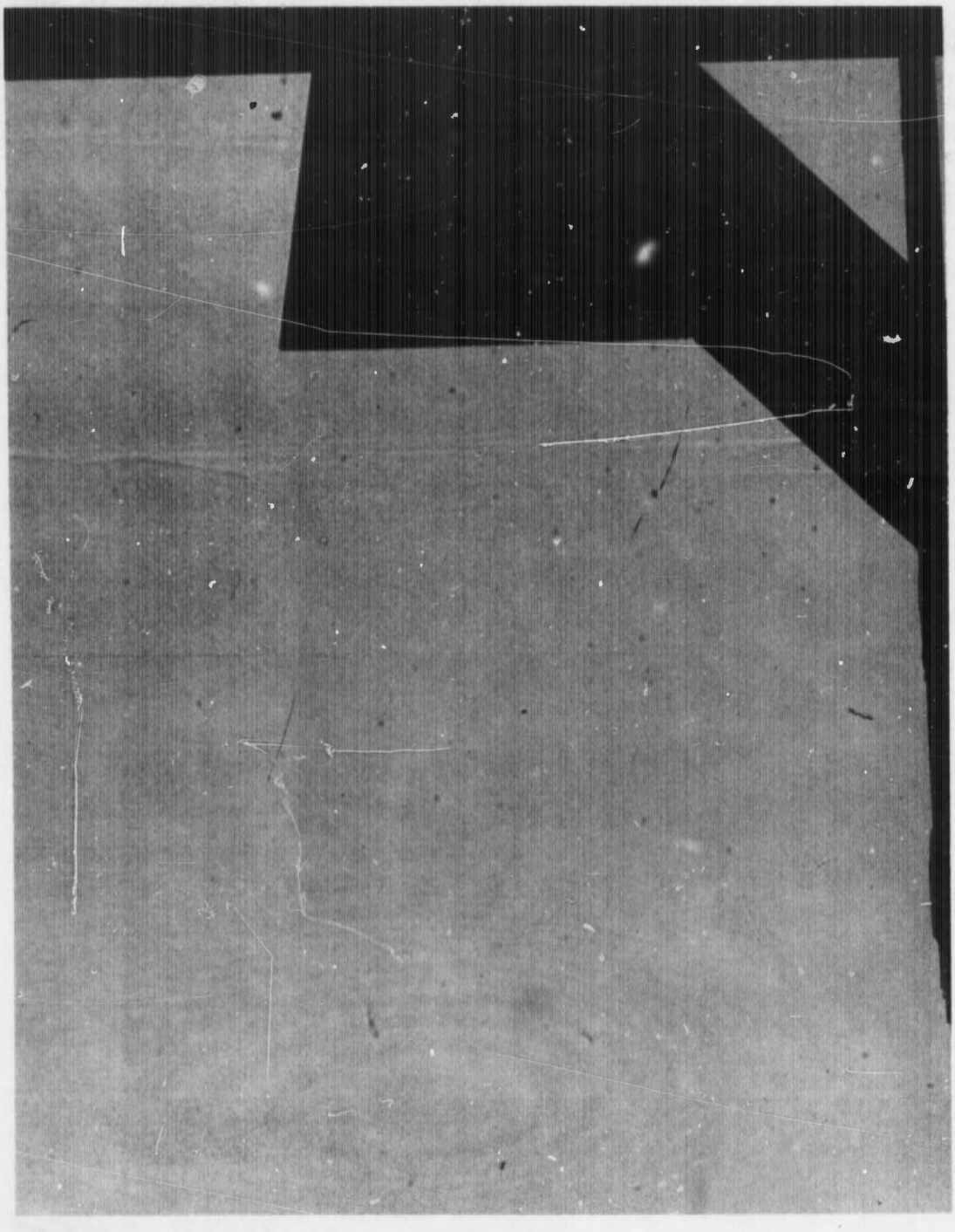

FIG. 20 CONT.
M. $M_1 = 5.1$, $M_s = 4.21$

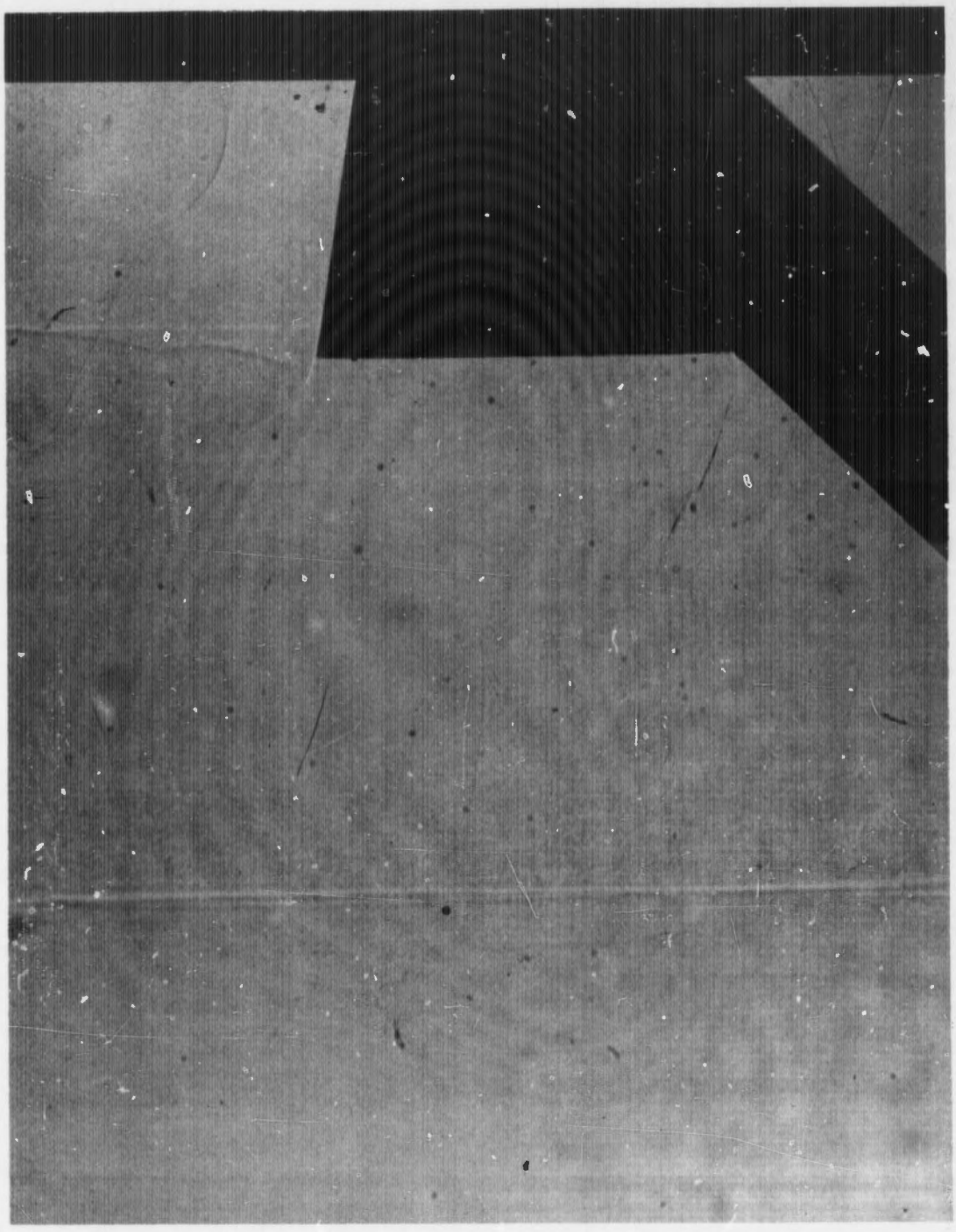

FIG. 20 CONT.
N. $M_1 = 5.1$, $M_s = 5.00$

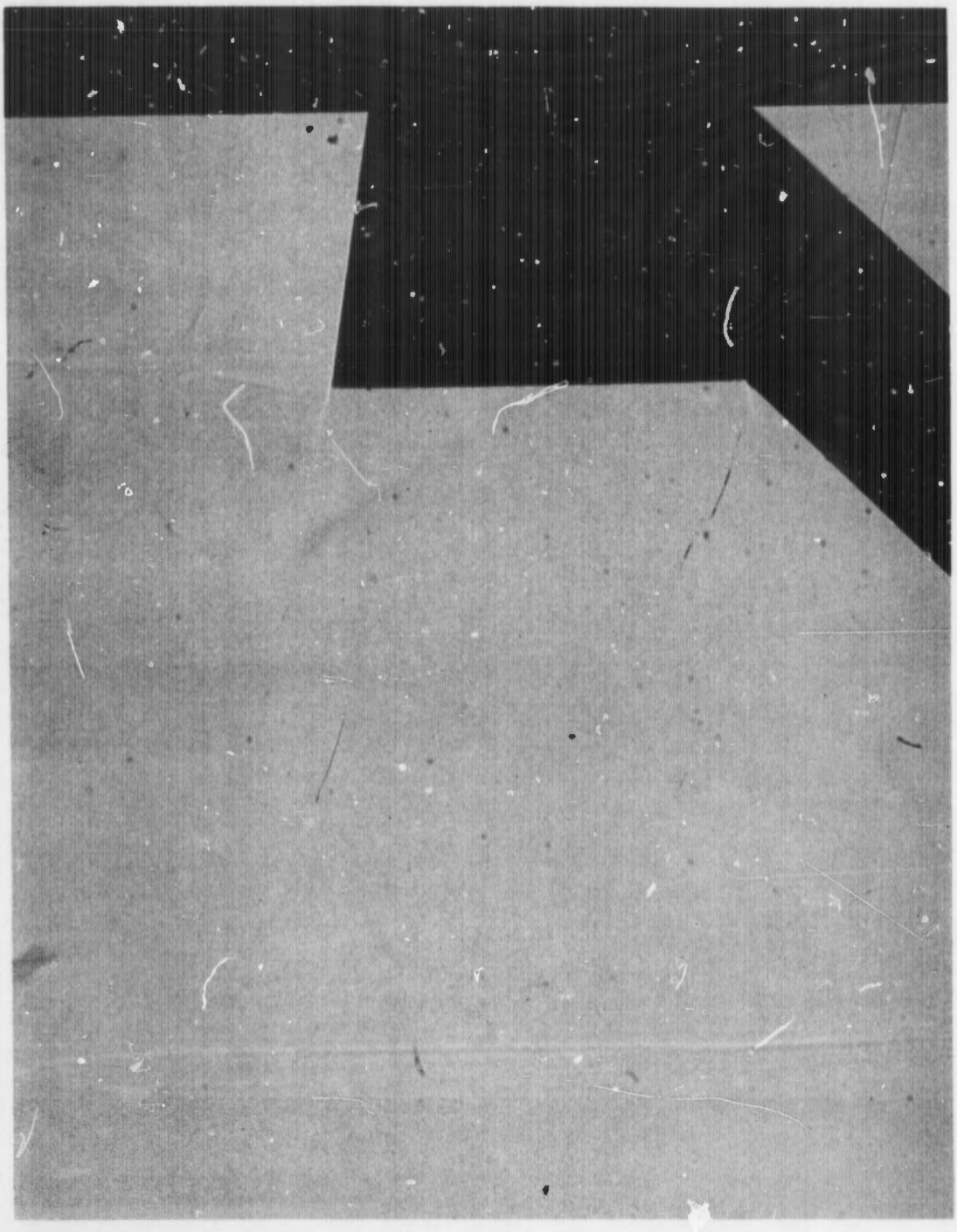

FIG. 20 CONT.

O. $M_1 = 5.1$, $M_s = 5.13$

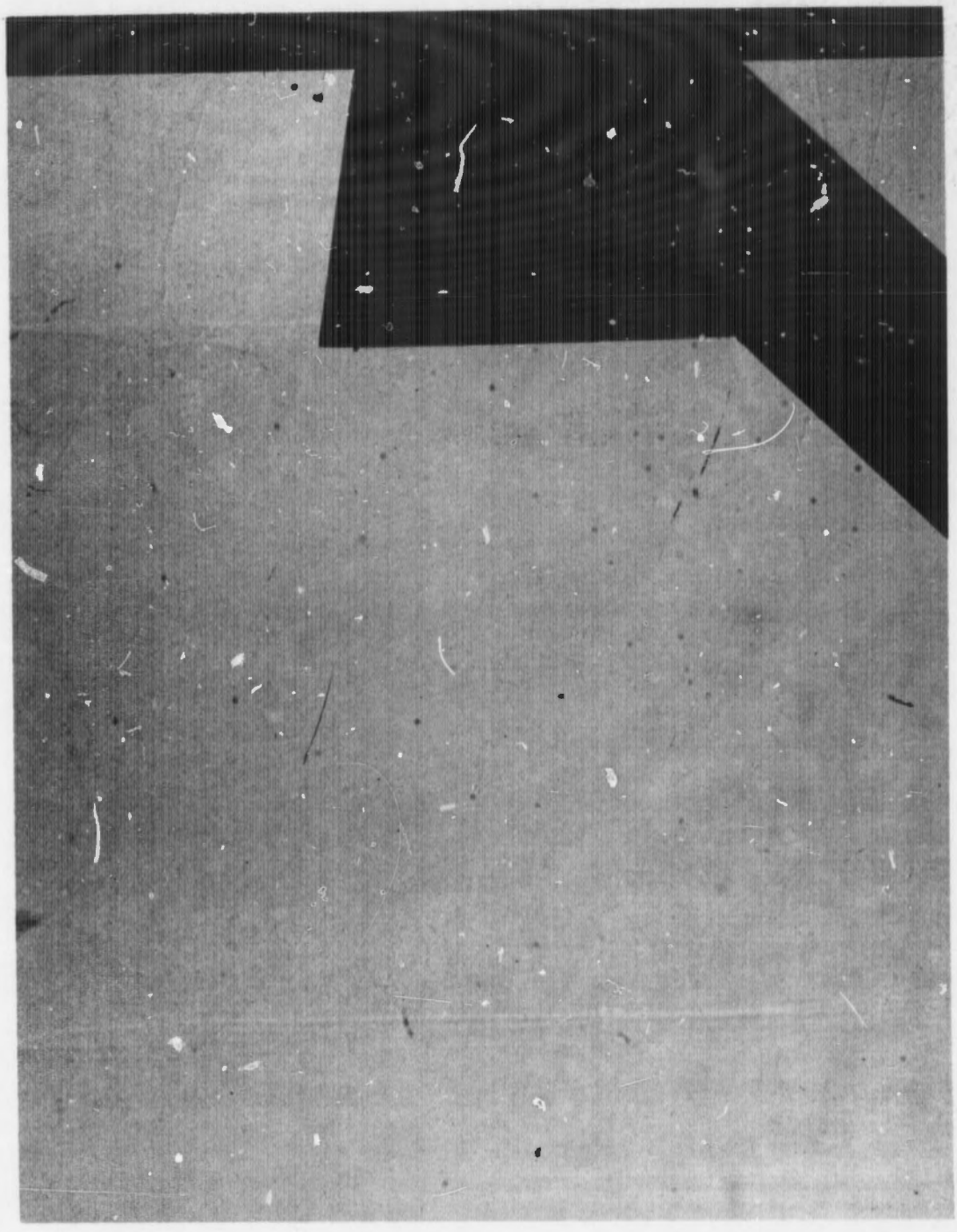

FIG. 20 CONT.
P. $M_j = 5.1$, $M_s = 5.17$

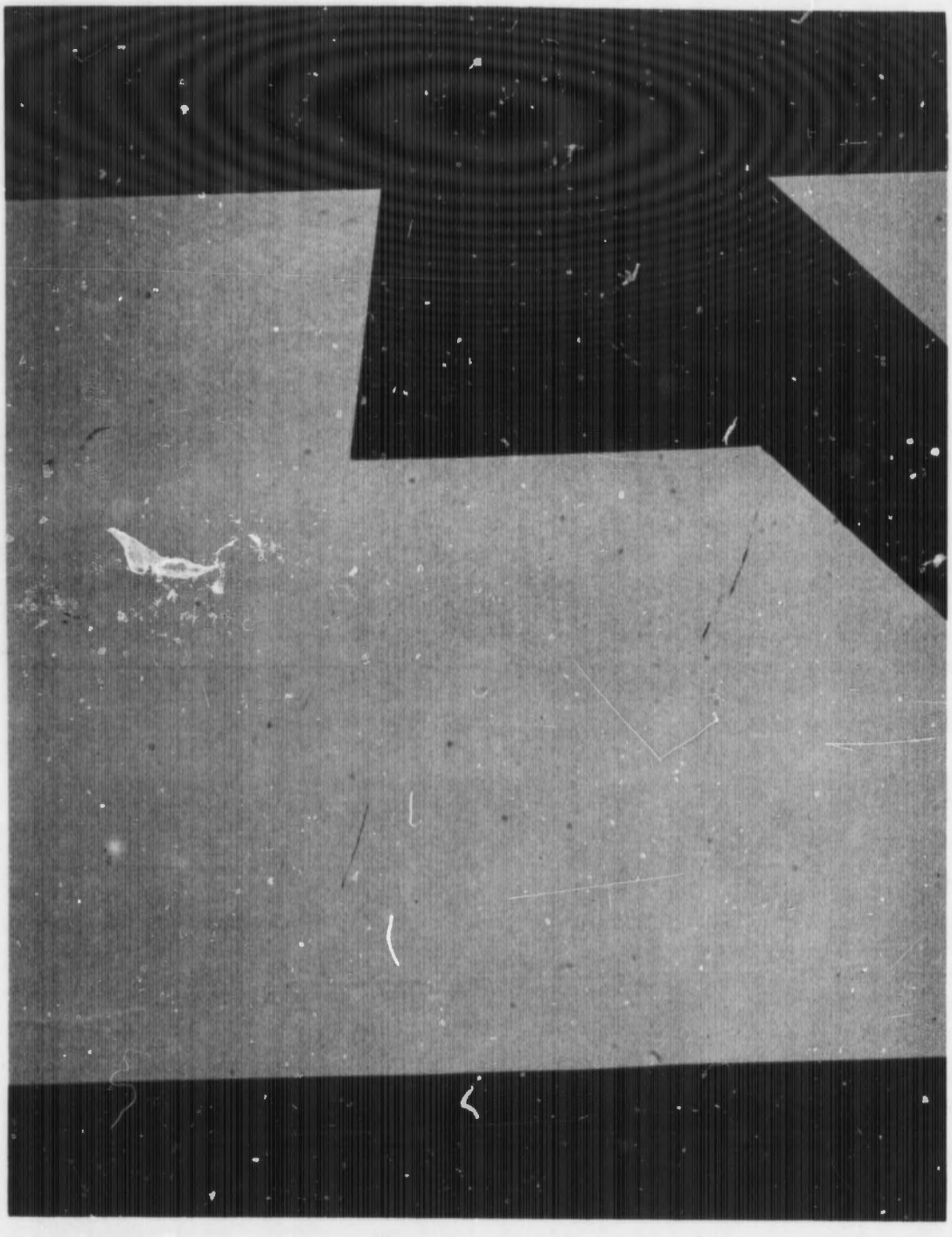

FIG. 20 CONT.
Q. $M_1 = 6.5$, $M_s = 4.31$

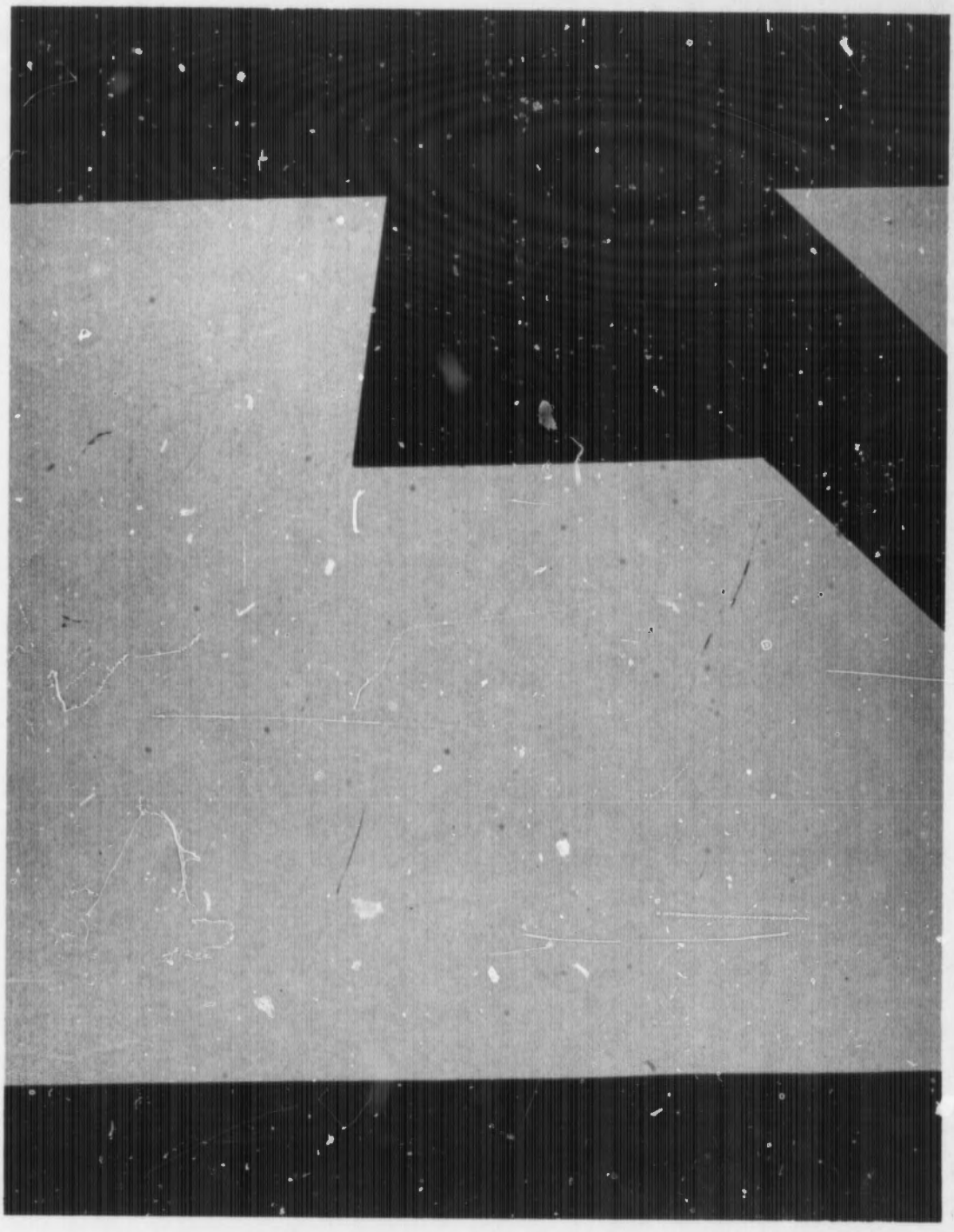

FIG. 20 CONT.
R. $M_j = 6.5$, $M_s = 5.98$

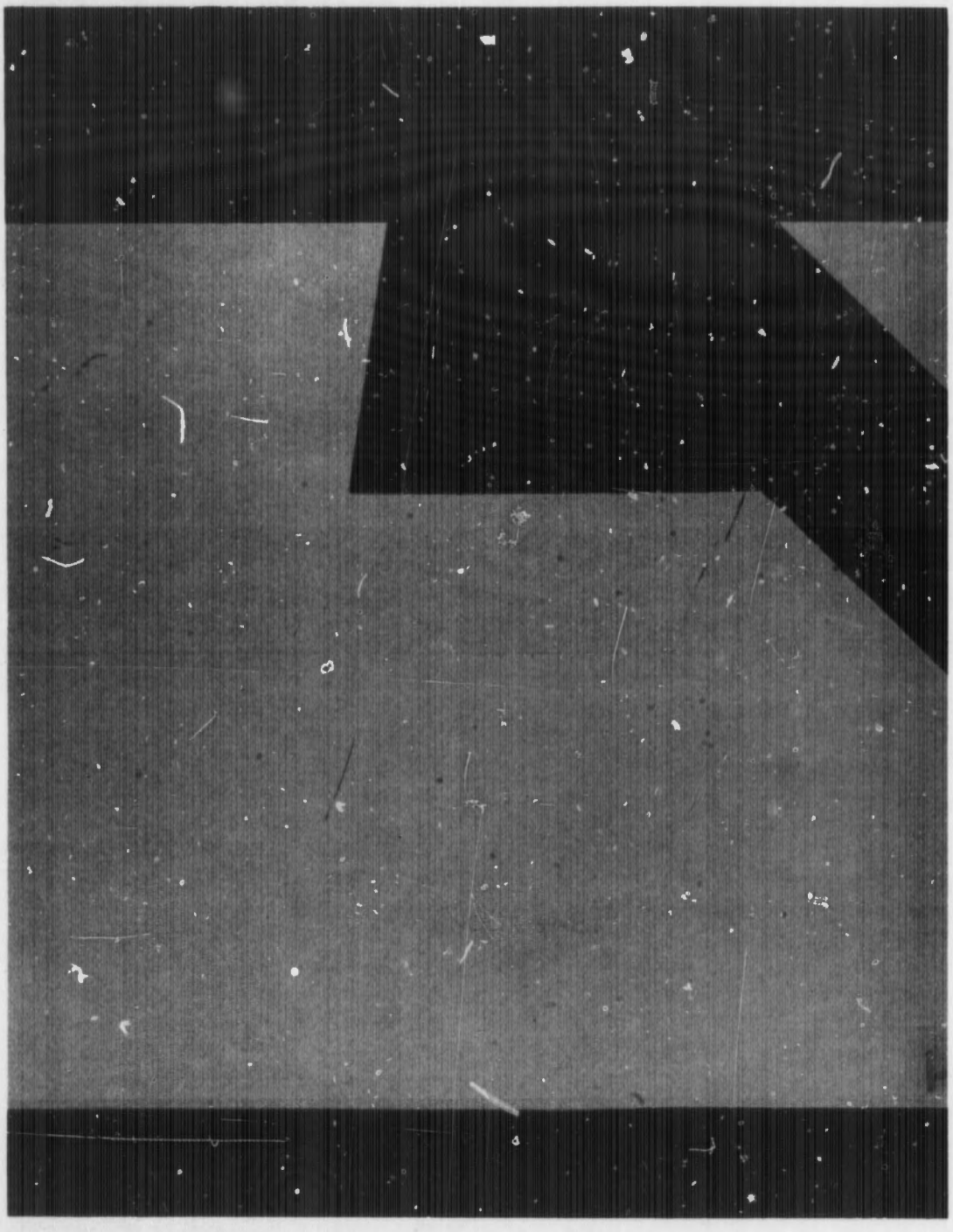

FIG. 20 CONT.
S. $M_1 = 6.5$, $M_s = 7.20$

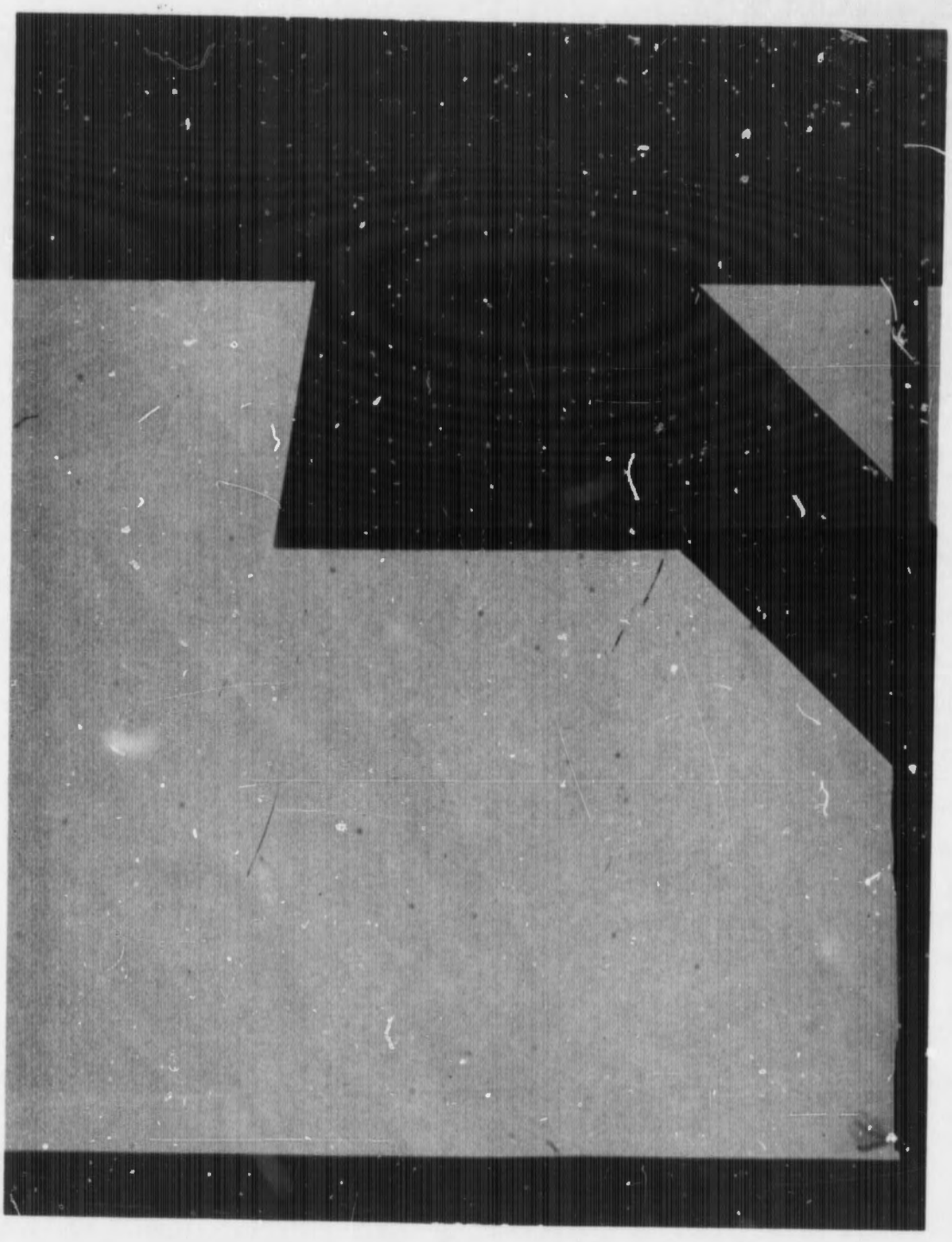

FIG. 20 CONT.
T. $M_j = 6.5$, $M_s = 7.48$

UNCLASSIFIED

Security Classification

DOCUMENT CONTROL DATA - R&D

(Security classification of title, body of abstract and indexing annotation must be entered when the overall report is classified)

1. ORIGINATING ACTIVITY (Corporate author)
U. S. Naval Ordnance Laboratory
White Oak, Silver Spring, Maryland

2a. REPORT SECURITY CLASSIFICATION
UNCLASSIFIED

2b. GROUP

3. REPORT TITLE
Measurements of Blast-Induced Transient Pressures at the Base of a Cone in Supersonic Flow

4. DESCRIPTIVE NOTES (Type of report and inclusive dates)

5. AUTHOR(S) (Last name, first name, initial)
Frank P. Baltakis
Gary D. Senechal

6. REPORT DATE	7a. TOTAL NO. OF PAGES	7b. NO. OF REFS
5 November 1969	60	5

8a. CONTRACT OR GRANT NO.	9a. ORIGINATOR'S REPORT NUMBER(S)
b. PROJECT NO. NOL 161/DASA	NOLTR 69-151
c.	9b. OTHER REPORT NO(S) (Any other numbers that may be assigned this report)
d.	

10. AVAILABILITY/LIMITATION NOTICES
This document is subject to special export controls and each transmittal to foreign governments or foreign nationals may be made only with prior approval of NOL.

11. SUPPLEMENTARY NOTES	12. SPONSORING MILITARY ACTIVITY
	Defense Atomic Support Agency

13. ABSTRACT

Transient pressures, induced by a head-on blast wave, have been measured at the base of a nine-degree half-angle cone in a supersonic stream using a wind-tunnel shocktube technique. Tests were conducted at free-stream Mach numbers of 3, 5 and 6.5 and at blast wave Mach numbers of 1.5 to 3, 2 to 5 and 4 to 8 at free-stream Mach numbers of 3, 5 and 6.5, respectively. Within the range of this experiment, the shock-induced base pressure was found to increase approximately in proportion to the blast wave Mach number squared. When expressed in ratio to the free-stream static pressure, the induced base pressure was found to decrease, approximately, linearly with increasing free-stream Mach number. At the free-stream/blast wave Mach number conditions of 3/3, 5/5 and 6.5/8 the respective induced base pressure to initial free-stream static pressure ratios were 5, 8 and 18.

DD FORM 1 JAN 64 1473

UNCLASSIFIED

Security Classification

UNCLASSIFIED

Security Classification

14. KEY WORDS	LINK A		LINK B		LINK C	
	ROLE	WT	ROLE	WT	ROLE	WT
Base Pressure						
Shock Interaction						
Cone						

INSTRUCTIONS

1. ORIGINATING ACTIVITY: Enter the name and address of the contractor, subcontractor, grantee, Department of Defense activity or other organization *(corporate author)* issuing the report.

2a. REPORT SECURITY CLASSIFICATION: Enter the overall security classification of the report. Indicate whether "Restricted Data" is included. Marking is to be in accordance with appropriate security regulations.

2b. GROUP: Automatic downgrading is specified in DoD Directive 5200.10 and Armed Forces Industrial Manual. Enter the group number. Also, when applicable, show that optional markings have been used for Group 3 and Group 4 as authorized.

3. REPORT TITLE: Enter the complete report title in all capital letters. Titles in all cases should be unclassified. If a meaningful title cannot be selected without classification, show title classification in all capitals in parenthesis immediately following the title.

4. DESCRIPTIVE NOTES: If appropriate, enter the type of report, e.g., interim, progress, summary, annual, or final. Give the inclusive dates when a specific reporting period is covered.

5. AUTHOR(S): Enter the name(s) of author(s) as shown on or in the report. Enter last name, first name, middle initial. If military, show rank and branch of service. The name of the principal author is an absolute minimum requirement.

6. REPORT DATE: Enter the date of the report as day, month, year; or month, year. If more than one date appears on the report, use date of publication.

7a. TOTAL NUMBER OF PAGES: The total page count should follow normal pagination procedures, i.e., enter the number of pages containing information.

7b. NUMBER OF REFERENCES: Enter the total number of references cited in the report.

8a. CONTRACT OR GRANT NUMBER: If appropriate, enter the applicable number of the contract or grant under which the report was written.

8b, 8c, & 8d. PROJECT NUMBER: Enter the appropriate military department identification, such as project number, subproject number, system numbers, task number, etc.

9a. ORIGINATOR'S REPORT NUMBER(S): Enter the official report number by which the document will be identified and controlled by the originating activity. This number must be unique to this report.

9b. OTHER REPORT NUMBER(S): If the report has been assigned any other report numbers *(either by the originator or by the sponsor)*, also enter this number(s).

10. AVAILABILITY/LIMITATION NOTICES: Enter any limitations on further dissemination of the report, other than those imposed by security classification, using standard statements such as:

(1) "Qualified requesters may obtain copies of this report from DDC."

(2) "Foreign announcement and dissemination of this report by DDC is not authorized."

(3) "U. S. Government agencies may obtain copies of this report directly from DDC. Other qualified DDC users shall request through _____."

(4) "U. S. military agencies may obtain copies of this report directly from DDC. Other qualified users shall request through _____."

(5) "All distribution of this report is controlled. Qualified DDC users shall request through _____."

If the report has been furnished to the Office of Technical Services, Department of Commerce, for sale to the public, indicate this fact and enter the price, if known.

11. SUPPLEMENTARY NOTES: Use for additional explanatory notes.

12. SPONSORING MILITARY ACTIVITY: Enter the name of the departmental project office or laboratory sponsoring *(paying for)* the research and development. Include address.

13. ABSTRACT: Enter an abstract giving a brief and factual summary of the document indicative of the report, even though it may also appear elsewhere in the body of the technical report. If additional space is required, a continuation sheet shall be attached.

It is highly desirable that the abstract of classified reports be unclassified. Each paragraph of the abstract shall end with an indication of the military security classification of the information in the paragraph, represented as *(TS), (S), (C), or (U)*

There is no limitation on the length of the abstract. However, the suggested length is from 150 to 225 words.

14. KEY WORDS: Key words are technically meaningful terms or short phrases that characterize a report and may be used as index entries for cataloging the report. Key words must be selected so that no security classification is required. Identifiers, such as equipment model designation, trade name, military project code name, geographic location, may be used as key words but will be followed by an indication of technical context. The assignment of links, roles, and weights is optional.

UNCLASSIFIED

Security Classification